

1  
2  
3  
4  
5  
6  
7  
8  
9  
10  
11  
12  
13  
14  
15  
16  
17  
18  
19  
20  
21  
22  
23  
24  
25  
26  
27  
28  
29

# Summer fluxes of methane and carbon dioxide from a pond and floating mat in a continental Canadian peatland

M. Burger<sup>1,2</sup>, S. Berger<sup>1,2</sup>, I. Spangenberg<sup>1,2</sup> and C. Blodau<sup>1,2</sup>

[1] Ecohydrology and Biogeochemistry Group, Institute of Landscape Ecology, University of Münster, Germany

[2] School of Environmental Sciences, University of Guelph, Canada

*Correspondence to:* C. Blodau (christian.blodau@uni-muenster.de)

## Abstract

Ponds smaller than 10000 m<sup>2</sup> likely account for about one third of the global lake perimeter. The release of methane (CH<sub>4</sub>) and carbon dioxide (CO<sub>2</sub>) from these ponds is often high and significant on the landscape scale. We measured CO<sub>2</sub> and CH<sub>4</sub> fluxes in a temperate peatland in southern Ontario, Canada, in summer 2014 along a transect from the open water of a small pond (847 m<sup>2</sup>) towards the surrounding floating mat (5993 m<sup>2</sup>) and in a peatland reference area. We used a high-frequency closed chamber technique and distinguished between diffusive and ebullitive CH<sub>4</sub> fluxes. CH<sub>4</sub> fluxes and CH<sub>4</sub> bubble frequency increased from a median of 0.14 (0.00 to 0.43) mmol m<sup>-2</sup> h<sup>-1</sup> and 4 events m<sup>-2</sup> h<sup>-1</sup> on the open water to a median of 0.80 (0.20 to 14.97) mmol m<sup>-2</sup> h<sup>-1</sup> and 168 events m<sup>-2</sup> h<sup>-1</sup> on the floating mat. The mat was a summer hot spot of CH<sub>4</sub> emissions. Fluxes were one order of magnitude higher than at an adjacent peatland site. During daytime the pond was a net source of CO<sub>2</sub> equivalents to the atmosphere amounting to 0.13 (-0.02 to 1.06) g CO<sub>2</sub> equivalents m<sup>-2</sup> h<sup>-1</sup>, whereas the adjacent peatland site acted as a sink of -0.78 (-1.54 to 0.29) g CO<sub>2</sub> equivalents m<sup>-2</sup> h<sup>-1</sup>. The photosynthetic CO<sub>2</sub> uptake on the floating mat did not counterbalance the high CH<sub>4</sub> emissions, which turned the floating mat into a strong net source of 0.21 (-0.11 to 2.12) g CO<sub>2</sub> equivalents m<sup>-2</sup> h<sup>-1</sup>. This study highlights the large small-scale variability of CH<sub>4</sub> fluxes and CH<sub>4</sub> bubble frequency at the peatland-pond interface and the importance of the often large ecotone areas surrounding small ponds as a source of greenhouse gases to the atmosphere.

## 1    **1.    Introduction**

2    Inland waters play a significant role in the global carbon cycle although covering only 3.7 %  
3    of the Earth's land surface (Bastviken et al., 2011; Raymond et al., 2013; Tranvik et al.,  
4    2009). They transport and sequester autochthonous and terrestrially derived carbon and are  
5    also sources of carbon dioxide (CO<sub>2</sub>) and methane (CH<sub>4</sub>) to the atmosphere (Cole et al., 2007;  
6    Tranvik et al., 2009). Global estimates of CO<sub>2</sub> and CH<sub>4</sub> emissions from inland waters have  
7    recently been corrected upward to 2.1 Pg C yr<sup>-1</sup> as CO<sub>2</sub> (Raymond et al., 2013) and 0.65 Pg C  
8    yr<sup>-1</sup> as CH<sub>4</sub> (Bastviken et al., 2011). Together they are similar to the net carbon uptake by  
9    terrestrial ecosystems of  $-2.5 \pm 1.3$  Pg C yr<sup>-1</sup> and to approximately one third of the  
10    anthropogenic CO<sub>2</sub> emissions (Ciais et al., 2013).

11    Small aquatic systems may be particularly important in this respect (Downing, 2010).  
12    According to high-resolution satellite imagery analyzed by Verpoorter et al. (2014), 77 % of  
13    the total 117 million lakes belong to the smallest detectable size category of 2000 to 10000 m<sup>2</sup>  
14    lake area. These waters only contribute 7 % to the area but 32 % to the total lake perimeter  
15    (Verpoorter et al., 2014). Numerous processes were found to proceed faster in small aquatic  
16    systems than in larger ones. Sequestration rates of organic carbon (Downing, 2010; Downing  
17    et al., 2008), the concentrations of CH<sub>4</sub>, CO<sub>2</sub>, and dissolved organic carbon (DOC) in the  
18    water column (Bastviken et al., 2004; Juutinen et al., 2009; Kelly et al., 2001; Kortelainen et  
19    al., 2006; Xenopoulos et al., 2003), and CH<sub>4</sub> and CO<sub>2</sub> emissions from the water to the  
20    atmosphere increase with decreasing lake size (Juutinen et al., 2009; Kortelainen et al., 2006;  
21    Michmerhuizen et al., 1996; Repo et al., 2007).

22    Small and shallow lakes and ponds are common in flat northern glacial landscapes and  
23    abundant in peatland areas, where 20 to 30 % of the world's soil organic carbon is stored  
24    (Turunen et al., 2002). CO<sub>2</sub> emissions from peatland ponds were reported to be in the same  
25    order of magnitude than net uptake of CO<sub>2</sub> by the peatland vegetation (Dinsmore et al., 2009;  
26    Hamilton et al., 1994). CH<sub>4</sub> emissions from open waters generally exceed CH<sub>4</sub> fluxes from  
27    vegetated areas by a factor 3 to 25 (Hamilton et al., 1994; McLaughlin and Webster, 2014;  
28    Trudeau et al., 2013). Small and shallow peatland ponds have been generally found to be  
29    particular strong emitters of the gas (McEnroe et al., 2009; Trudeau et al., 2013). Moreover,  
30    CH<sub>4</sub> and CO<sub>2</sub> emissions from open waters can be significant on the landscape scale despite  
31    their often small area (Dinsmore et al., 2010; Juutinen et al., 2013). Pelletier et al. (2014)  
32    estimated that a pond cover of > 37 % could convert a northern peatland from a carbon sink  
33    into a carbon source. Such findings are relevant as Hamilton et al. (1994) and Trudeau et al.  
34    (2013) reported a pond cover of 8 to 12 % and 42 % in fens and bogs in northern Canada. The  
35    authors suspected a contribution of aquatic CH<sub>4</sub> fluxes to landscape CH<sub>4</sub> fluxes of 30 % and  
36    79 %, respectively. Very high CH<sub>4</sub> emissions have also been reported from a floating mat on a

1 thermokarst pond and a floating mat within a bog pond (Flessa et al., 2008; Sugimoto and  
2 Fujita, 1997). Juutinen et al. (2013) documented highest CH<sub>4</sub> fluxes from a wet lawn adjacent  
3 to a small fen lake compared to the lake itself and fen lawns farther away from the small lake.  
4 Fluxes of CH<sub>4</sub> and CO<sub>2</sub> from ponds are controlled by environmental and biotic factors.  
5 Atmospheric CH<sub>4</sub> fluxes are controlled by microbial production and oxidation of CH<sub>4</sub> within  
6 peat, sediment and surface water and the diffusive, ebullitive, and plant-mediated transport to  
7 the atmosphere (Bastviken et al., 2004; Bridgman et al., 2013; Carmichael et al., 2014). CO<sub>2</sub>  
8 exchange is driven by the interplay of heterotrophic and autotrophic respiration and by  
9 photosynthesis of aquatic macrophytes and algae. Both gas fluxes are linked to the quantity  
10 and quality of organic and inorganic carbon supplied from the surrounding catchment  
11 (Huttunen et al., 2002; Macrae et al., 2004; Tranvik et al., 2009). They are also related to  
12 temperature, wind speed and air pressure (e. g. Trudeau et al., 2013; Varadharajan and  
13 Hemond, 2012; Wik et al., 2013). Ebullition appears to be of particular importance for CH<sub>4</sub>  
14 release to the atmosphere (Walter et al., 2006; Wik et al., 2013) and varies on scales of several  
15 tens to hundreds of meters (Bastviken et al., 2004; Wik et al., 2013). Emissions of CH<sub>4</sub>  
16 emissions are generally lower in the pelagic than in the littoral zone, where plant habitats  
17 further influence fluxes (Juutinen et al., 2001; Larmola et al., 2004). On the other hand,  
18 Trudeau et al. (2013) found 2.5 to 5 times lower CH<sub>4</sub> fluxes at the border of fen pools than in  
19 the center of the pools with areas of 60 and 200 m<sup>2</sup>. Measurements in this study were carried  
20 out in a situation where pool size has been historically increasing at the expense of  
21 surrounding terrestrial areas.

22 Despite this progress, knowledge on the temporal and spatial variability of CH<sub>4</sub> and CO<sub>2</sub>  
23 fluxes within small pond systems is limited. We know, for example, little about the CH<sub>4</sub> and  
24 CO<sub>2</sub> exchange of transition zones between ponds and surrounding peatlands, which can be  
25 especially important due to the high perimeter to area ratio of small ponds (Verpoorter et al.,  
26 2014). It is important to consider the net effect of different microforms of peatlands by taking  
27 into account the global warming potentials, as CH<sub>4</sub> emissions may easily offset carbon sinks  
28 in ponds. To gain more insight into these issues we investigated the summer atmospheric CO<sub>2</sub>  
29 and CH<sub>4</sub> exchange of open water, a floating mat and an adjacent peatland area in a temperate  
30 peatland in southern Ontario, Canada. In particular we tested the hypothesis that (I) ebullitive  
31 and diffusive CH<sub>4</sub> fluxes increase from the open water towards a floating mat surrounding the  
32 pond. We examined further the expectation that (II) CH<sub>4</sub> and CO<sub>2</sub> effluxes from the system  
33 increases with temperature and wind speed, and investigated if falling air pressure raises CH<sub>4</sub>  
34 fluxes. To assess the importance of the pond system for the greenhouse gas balance we  
35 calculated the net radiative forcing of the investigated peatland microforms.

## 1 2 **Materials and methods**

### 2 **2.1 Study site**

3 Wylde Lake Bog is located in the southeastern part of the Luther Marsh Wildlife Management  
4 Area (43°54.667' N, 80°24.022' W) (Fig. 1) at about 490 m above sea level and has an area of  
5 approximately 7.8 km<sup>2</sup>. A 600 cm deep profile analyzed by Givelet et al. (2003) documented  
6 clay-rich sediments up to 560 cm depth, gyttja from 560 to 490 cm, fen peat from 490 to  
7 approximately 300 cm and bog peat above 300 cm depth. The peatland is dominated by  
8 mosses, graminoids, dwarf shrubs and sporadic trees, and a pronounced hummock-hollow-  
9 microtopography. Common in the peatland are *Sphagnum magellanicum*, *S. capillifolium*,  
10 *Carex disperma* and *Chamaedaphne calyculata* and on the floating mat *S. angustifolium*, *S.*  
11 *magellanicum* and *Rhynchospora alba*. The plant species composition of the study site is  
12 given in the Supplementary Information (Table S1). The vicinity of the pond is characterized  
13 by small open and larger treed areas dominated by *Larix laricina* and *Picea mariana*. The  
14 pond (Fig. 1) has an area of 847 m<sup>2</sup> and a depth of 0.3 to 0.8 m. The interface between the  
15 water column and the organic deposits is not clearly delimited but consists of a transition zone  
16 with suspended organic material. It likely has changed in size, depth, and shape throughout  
17 the last decades. Sandilands (1984) reported that larger, adjacent Wylde Lake shrunk from  
18 0.4 km<sup>2</sup> in 1928 to 0.05 km<sup>2</sup> in 1984. The floating mat (Fig. 1) surrounding the pond has an  
19 area of approx. 5993 m<sup>2</sup>. Climate is temperate continental with a mean annual air temperature  
20 of about 6.7 °C, annual precipitation of 946 mm including 148 mm of snowfall, and an  
21 average frost-free period from May 7<sup>th</sup> to October 6<sup>th</sup> (1981 to 2010, Fergus Shand Dam,  
22 National Climate Data and Information Archive, 2014).

23

### 24 **2.2 Environmental variables**

25 Air temperature, relative humidity, wind speed, wind direction, photosynthetically active  
26 radiation (PAR) and precipitation were recorded at the study site by a HOBO U30 weather  
27 station (U30-NRC-SYS-B, Onset) (Supplementary Information, Table S2). Water temperature  
28 of the pond and the temperature of the floating mat were also continuously measured. Air  
29 pressure was recorded at a distance of 1.1 km from the study site (Supplementary  
30 Information, Table S2). In addition we qualitatively observed presence of algae in the pond  
31 and occasionally took pictures of the pond and algae.

32

### 33 **2.3 CH<sub>4</sub> and CO<sub>2</sub> flux measurements with closed chambers**

34 CH<sub>4</sub> and CO<sub>2</sub> fluxes of the pond and the floating mat were measured once a week from July  
35 10<sup>th</sup> to September 29<sup>th</sup>, 2014 between 1 pm ± 1.5 hours and 5 pm ± 1.5 hours using closed

1 chambers designed according to Drösler (2005). We used a long wooden board floating on  
2 air-filled canisters on the pond-end ('floating boardwalk') to do our measurements and to  
3 minimize pressure on the ground (Supplementary Information, Fig. S1). The other end was  
4 secured at the drier end of the floating mat. The cylindrical, transparent Plexiglas chambers  
5 had a basal area of 0.12 m<sup>2</sup> and a height of 0.40 m. They were equipped with 2 or 3 fans  
6 (Micronel Ventilator D341T012GK-2, BEDEK GmbH) to circulate the air, a  
7 photosynthetically active radiation (Photosynthetic Light (PAR) Smart Sensor, S-LIA-M002,  
8 Onset ) and an air temperature sensor (RH Smart Sensor, S-THB-M002, Onset; see also  
9 Supplementary Information for further information on instrumentation, Table S2). To  
10 compensate for air pressure differences, we attached a vent tube, 12 cm long and 7 mm inner  
11 diameter, to the chamber (Davidson et al., 2002). Transparent chambers were used to measure  
12 net ecosystem exchange (NEE) and cooled with up to 6 ice packs depending on ambient  
13 temperature to ensure a temperature change of less than 1°C during the chamber closure. For  
14 the measurements chamber orientation was adjusted to avoid shading of the chamber basal  
15 area by the ice packs. Ecosystem respiration (ER) was measured with chambers covered with  
16 reflective insulation foil. On the water, chambers were operated with a Styrofoam float  
17 (0.80 m × 0.61 m × 0.08 m). The chamber walls extended 10 cm below the water surface as  
18 recommended by Soumis et al. (2008). CH<sub>4</sub> and CO<sub>2</sub> concentrations were quantified with an  
19 Ultraportable Greenhouse Gas Analyzer (915-001, Los Gatos Research) at a temporal  
20 resolution of 1 s. According to the manufacturer, a single data point has a precision of < 2 ppb  
21 for CH<sub>4</sub> and < 300 ppb for CO<sub>2</sub>. Stability of the calibration was checked in March and August  
22 2014. The air was circulated between the chamber and the analyzer through low-density  
23 polyethylene tubes of 5 m length with an inner diameter of 2 mm and a water vapor trap.  
24 Using this setup it took 36 s until the sampling cell of the analyzer was fully flushed and the  
25 concentration had stabilized.

26 Flux measurements on the open water were carried out in 6 locations with increasing distance  
27 of 0.7 m to 4.6 m to the floating mat (Supplementary Information, Table S3). A float with  
28 chamber was secured in place by a couple of telescopic poles that were rigidly connected to  
29 the floating boardwalk. This way we avoided a drifting of the chamber. On the floating mat  
30 the chambers were placed on cylindrical PVC collars with a height of 25 cm. Collars had been  
31 inserted into the mat to depths of approximately 15 cm prior to the first measurement. Each  
32 sampling day fluxes were measured at least once with the transparent and with the radiation-  
33 shielded chamber, for 5 min on the pond and 3 min on the floating mat, by placing the  
34 chamber gently as soon as the concentration reading was stable. When CH<sub>4</sub> concentrations  
35 increased sharply within the first 60 s of the measurement due to CH<sub>4</sub> bubble release caused  
36 by the positioning of the chamber, the measurement was discarded and repeated. Fluxes were

1 also quantified at a peatland site in the north-northeast of the pond (Fig. 1) with the same  
2 approach, every other week from July 4<sup>th</sup> until October 1<sup>st</sup>, 2014, on 12 measuring plots  
3 covering hummocks, hollows and lawns. In this area of the peatland, hummocks cover 90 %  
4 of the area, hollows 9.8 % and lawns 0.2 % of the area.

5 Fluxes were calculated based on the gas concentration change in the chamber over time using  
6 linear regression and the ideal gas law, mean air temperature inside the chamber and the  
7 corresponding half hour mean air pressure. The chamber volume was calculated for each  
8 measurement depending on the number of ice packs, immersion depth on the pond and mean  
9 vegetation height on the floating mat. The first 40 s after chamber deployment were discarded  
10 for flux calculation due to the response time of the concentration measurement. If the slope  
11 was not significantly different from 0 (F test,  $\alpha = 0.05$ ), the flux was set to 0. Concentration  
12 change over time was only  $< 3$  ppm CO<sub>2</sub> and  $< 0.1$  ppm CH<sub>4</sub> in 12 % of flux measurements.  
13 These measurements resulted in fluxes close to 0 with  $R^2 < 0.8$ . Following Repo et al. (2007),  
14 we included them in the data set because their exclusion would have biased the results by  
15 increasing the median diffusive fluxes by 52 % (CO<sub>2</sub>) and 12 % (CH<sub>4</sub>).

16 Due to the high temporal resolution of concentration measurements, we were able to quantify  
17 CH<sub>4</sub> fluxes with and without bubbles. When the CH<sub>4</sub> concentrations evolved linearly with a  
18 constant slope we used linear regression over the entire time of sampling; when the initial  
19 concentration trend was interrupted by one or several sharp increases in slope, followed by a  
20 return to the initial slope (Supplementary Information, Fig. S1), we used piecewise linear  
21 fitting for each of the linear segments (Goodrich et al., 2011). According to Goodrich et al.  
22 (2011) and Xiao et al. (2014), we define sharp increases in slope as ebullitive CH<sub>4</sub> fluxes and  
23 all others as diffusive or continuous flux of micro-bubbles. Time-weighted averages including  
24 diffusive and ebullitive flux segments were calculated. We also computed the CH<sub>4</sub> bubble  
25 frequency in events  $m^{-2} h^{-1}$  as the number of bubble events divided by measuring time and  
26 area. In order to evaluate the contribution of ebullitive CH<sub>4</sub> flux to the total CH<sub>4</sub> flux, the CH<sub>4</sub>  
27 release of each event in  $\mu\text{mol}$  was calculated by multiplying the ebullitive flux with the  
28 duration of the event and the basal area of the chamber.

29 For comparisons of NEE between sites and with time, we used the maximum NEE defined as  
30 light-saturated at PAR levels  $> 1000 \mu\text{mol m}^{-2} \text{s}^{-1}$  according to a study by Larmola et al.  
31 (2013). We further calculated the net exchange of CO<sub>2</sub> equivalents for each flux  
32 measurement. To this end, the CH<sub>4</sub> flux was converted into CO<sub>2</sub> equivalents by multiplying  
33 the mass flux with the global warming potential of 28 for a 100 year time horizon (Myhre et  
34 al., 2013). Subsequently, the CH<sub>4</sub> flux in CO<sub>2</sub> equivalents and the maximum NEE were  
35 summed up.

36

## 2.4 CO<sub>2</sub> concentration measurements and gradient flux calculations

To obtain estimates of daily time series of CO<sub>2</sub> concentration and fluxes, concentrations of CO<sub>2</sub> in the surface water of the pond and in the air were measured with calibrated non-dispersive infrared absorption sensors (CARBOCAB, GMP222, Vaisala) in the range up to 10000 ppm and with an accuracy of  $\pm 150$  ppm plus 2 % of the reading. The probe was enclosed in CO<sub>2</sub> permeable silicone tubes, as already used by Estop et al. (2012) in peats, and attached to a floating platform at a depth of approximately 18 cm and a distance of 3.2 m from the pond margin. In water equilibration time to 90% of dissolved concentration was approximately one hour when concentration increased but more delayed when it fell (Supplementary Information, Fig. S3). The platform also carried the data logger (MI70, Vaisala). Another silicon-covered sensor measured air CO<sub>2</sub> concentrations at 0.3 m above the water surface. Concentration was recorded every 15 min and CO<sub>2</sub> flux across the air-water interface estimated according to the boundary layer equation approach (Supplementary Information). Due to frequent failures of the sensors with increased humidity in the sensor head and overheating of the data logger, CO<sub>2</sub> fluxes were only calculated for 5 and 3 exemplary days in July and September, respectively. During these periods sensor functioning was stable.

## 2.5 CH<sub>4</sub> and CO<sub>2</sub> concentrations and diffusive fluxes in the sediment

Dissolved CH<sub>4</sub> and CO<sub>2</sub> concentrations at the sediment-water-interface were determined with pore water peepers of 60 cm length and 1 cm resolution as developed by Hesslein (1976). The chambers were filled with deionized water, covered with a nylon membrane of 0.2  $\mu\text{m}$  pore size, installed at four locations randomly distributed across the pond on August 21<sup>st</sup>, 2014 and sampled on September 25<sup>th</sup> and 29<sup>th</sup>, 2014. The pH of every other cell was measured in the field and a sample of 0.5 mL from each chamber filled into a vial containing 20  $\mu\text{L}$  of 4 M hydrochloric acid (HCl). CO<sub>2</sub> and CH<sub>4</sub> concentrations in the headspace of the vials were determined with an SRI 8610C gas chromatograph equipped with a methanizer and a flame ionization detector on the day after sampling. The original CO<sub>2</sub> and CH<sub>4</sub> concentrations in the pore water were calculated by using the measured headspace concentrations, Henry's law with temperature corrected Henry's law constants (Sander, 1999) and the ideal gas law. Diffusive fluxes of CO<sub>2</sub> and CH<sub>4</sub> towards the sediment-water interface were calculated with Fick's first law and diffusion coefficients in water  $D_w$  corrected for an assumed sediment temperature of 15°C (CH<sub>4</sub>:  $1.67 \cdot 10^{-5} \text{ cm}^2 \text{ s}^{-1}$ ; CO<sub>2</sub>:  $1.87 \cdot 10^{-5} \text{ cm}^2 \text{ s}^{-1}$ ) and assuming a porosity  $n$  of 0.9. The effect of porosity on the sediment diffusion coefficient was accounted for by multiplying  $D_w$  with a factor  $n^2$  (Lerman, 1978). We further calculated a theoretical temperature- and depth-dependent threshold of bubble formation using Henry's law,

1 correcting Henry's law constant for a temperature of 15°C, and assuming a partial pressure of  
2 N<sub>2</sub> in the pore water of 0.8 atm or 0.5 atm. The assumption here is that bubble formation is  
3 possible when the partial pressure of CH<sub>4</sub> and remaining N<sub>2</sub> exceeds atmospheric and water  
4 pressure in the anoxic sediment. In addition we sampled occasionally gas bubbles trapped in  
5 an algal mat that was present on the pond until August 12<sup>th</sup>.  
6

## 7 **2.6 Statistical analyses**

8 Statistical analyses were performed with R, version 3.1.2 (R Core Team, 2014). All datasets  
9 were checked for normality with the Shapiro-Wilk normality test at a confidence level of  
10  $\alpha = 0.05$ . To investigate statistical differences of a continuous variable between two or more  
11 groups, we used the non-parametric Kruskal-Wallis rank sum test ( $\alpha = 0.05$ ) and if applicable  
12 afterwards the multiple comparison test after Kruskal-Wallis ( $\alpha = 0.05$ ) since none of the  
13 datasets were normally distributed. For the investigation of relationships between two  
14 continuous variables, we used Spearman's rank correlation ( $\alpha = 0.05$ ). Due to visually  
15 different dynamics of the gas fluxes from July 10<sup>th</sup> to August 7<sup>th</sup> (here called "mid summer")  
16 compared to August 15<sup>th</sup> to September 29<sup>th</sup> (here called "late summer"), correlations with  
17 environmental variables were examined for the whole period as well as the two subperiods.  
18  
19

## 20 **3 Results**

### 21 **3.1 Weather and pond conditions**

22 Three distinct periods of weather occurred. From July 10<sup>th</sup> until September 10<sup>th</sup>, 2014, air  
23 temperatures remained high with a mean ( $\pm$  standard deviation) of  $17.0 \pm 2.7$  °C (Fig. 2).  
24 Most days were sunny with some passing clouds. From September 11<sup>th</sup> to September 22<sup>nd</sup>,  
25 2014, mean air temperature had cooled to  $10.2 \pm 2.8$  °C and the first frost occurred on  
26 September 14<sup>th</sup> (Fig. 2). From September 23<sup>rd</sup> to 29<sup>th</sup>, mean air temperature was  $13.2 \pm 7.6$  °C  
27 with a high daily amplitude from  $3.7 \pm 1.3$  °C to  $24.3 \pm 1.5$  °C and wind speed was low with a  
28 mean of  $0.14 \pm 0.31$  m s<sup>-1</sup> (Fig. 2). Major storms with maximum wind speeds from 3 to 5.5 m  
29 s<sup>-1</sup> on July 23<sup>rd</sup>, July 28<sup>th</sup>, August 12<sup>th</sup>, September 6<sup>th</sup>, September 11<sup>th</sup> and September 21<sup>st</sup>  
30 were accompanied by air pressure decline to lows between 944 and 955 hPa. Often rainfall  
31 reached an intensity of 2.8 to 6.2 mm in the chosen 5 min time intervals (Fig. 2).

32 During the summer an algae mat developed in the pond that impeded water circulation (see  
33 Supplementary Information for visuals). This algae mat was irreversibly dissolved with the  
34 storm on August 12<sup>th</sup>. As gas exchange with the atmosphere distinctly differed before and



1 after this event, we used the storm as a distinction between “mid summer” and “late summer”  
2 conditions throughout the analysis.

### 3 4 **3.2 CH<sub>4</sub> and CO<sub>2</sub> fluxes over time**

5 CH<sub>4</sub> fluxes from the pond were significantly lower in the period from July 10<sup>th</sup> until August  
6 7<sup>th</sup> with a median of 0.03 mmol m<sup>-2</sup> h<sup>-1</sup> compared to a median of 0.21 mmol m<sup>-2</sup> h<sup>-1</sup> from  
7 August 15<sup>th</sup> until September 29<sup>th</sup> (Kruskal-Wallis test,  $p < 0.001$ ,  $n = 159$ ) (Fig. 3 A). The  
8 highest median CH<sub>4</sub> flux, highest maximum flux, and largest variability were observed on  
9 August 15<sup>th</sup>, after the algal mat had been dissolved on August 12<sup>th</sup>. The bubble frequency  
10 varied between 0 and 30 events m<sup>-2</sup> h<sup>-1</sup> (Fig. 3 B) and the contribution of the ebullitive to the  
11 total CH<sub>4</sub> flux between 90 % in mid-July and 0 % in late September (Fig. 3 C). Efflux of CH<sub>4</sub>  
12 from the floating mat was variable but significantly higher in late summer with a median of  
13 0.80 mmol m<sup>-2</sup> h<sup>-1</sup> than in mid summer with a median of 0.22 mmol m<sup>-2</sup> h<sup>-1</sup> (Kruskal-Wallis  
14 test,  $p < 0.001$ ,  $n = 84$ ) (Fig. 4 A). The bubble frequency on the floating mat ranged from 0 to  
15 80 events m<sup>-2</sup> h<sup>-1</sup> and the contribution of ebullition to CH<sub>4</sub> flux from 0 to 88 % (Fig. 4 B and  
16 C). At the peatland site, CH<sub>4</sub> fluxes were similar over time with a median of 0.31 mmol  
17 m<sup>-2</sup> h<sup>-1</sup> and two very high individual fluxes in September and October (Fig. 5 A). The bubble  
18 frequency and contribution of ebullition to CH<sub>4</sub> flux ranged from 0 to 5 events m<sup>-2</sup> h<sup>-1</sup> and 0  
19 to 54 %, respectively (Fig. 5 B and C).

20 CO<sub>2</sub> fluxes from the pond in mid summer had a median of 0.11 mmol m<sup>-2</sup> h<sup>-1</sup> and were also  
21 significantly lower than the pond CO<sub>2</sub> fluxes in late summer with a median of 1.80 mmol  
22 m<sup>-2</sup> h<sup>-1</sup> (Kruskal-Wallis test,  $p < 0.001$ ,  $n = 159$ ) (Fig. 3 D). During 24 out of 55 individual  
23 measurements before August 15<sup>th</sup>, CO<sub>2</sub> exchange across the water-atmosphere interface was  
24 absent or CO<sub>2</sub> was taken up by the pond between 0 and -0.75 mmol m<sup>-2</sup> h<sup>-1</sup>. Subsequently  
25 CO<sub>2</sub> was net emitted. The median daytime ER of the floating mat was 6.77 mmol m<sup>-2</sup> h<sup>-1</sup> and  
26 the median of the maximum NEE -4.81 mmol m<sup>-2</sup> h<sup>-1</sup> (Fig. 4 D). Daytime ER at the peatland  
27 site varied between 2.61 to 36.93 mmol m<sup>-2</sup> h<sup>-1</sup> with a median of 11.98 mmol m<sup>-2</sup> h<sup>-1</sup> and  
28 tended to decrease towards fall (Fig. 5 D). The maximum NEE was quite constant from July  
29 until September with a median of -16.98 mmol m<sup>-2</sup> h<sup>-1</sup>.

30 The gradient method provided similar CO<sub>2</sub> fluxes in July and September with a median of  
31 1.99 mmol m<sup>-2</sup> h<sup>-1</sup> in July and 2.02 mmol m<sup>-2</sup> h<sup>-1</sup> in September (Supplementary Information,  
32 Fig. S2). The daily amplitude of fluxes determined with this method was 1.46 to 3.19 mmol  
33 m<sup>-2</sup> h<sup>-1</sup> in July and 1.41 to 1.86 mmol m<sup>-2</sup> h<sup>-1</sup> in September (Supplementary Information Fig.  
34 S2). Comparing results of floating chamber and gradient method, in July, when the algal mat  
35 on the pond was present, the daytime CO<sub>2</sub> fluxes obtained by the gradient method were 14-  
36 fold higher than the respective CO<sub>2</sub> fluxes measured with the floating chambers (Kruskal-

1 Wallis test,  $p < 0.001$ ,  $n = 189$ ). In September the results of gradient and chamber method  
2 were not significantly different.

### 3 4 **3.3 CO<sub>2</sub> and CH<sub>4</sub> concentrations and diffusion in the surface water and sediments**

5 CO<sub>2</sub> concentrations of the surface water of the pond were similar during the examined periods  
6 in July and September with a mean ( $\pm$  standard deviation) of  $114.8 \pm 33.1 \mu\text{mol L}^{-1}$  and  $132.0$   
7  $\pm 21.0 \mu\text{mol L}^{-1}$ , respectively (Fig. S2, Supplementary Information). In both periods we  
8 observed diurnal cycles of CO<sub>2</sub> concentrations covering a mean amplitude of  $83.5 \pm 16.3$   
9  $\mu\text{mol L}^{-1}$  (July) and  $62.0 \pm 3.1 \mu\text{mol L}^{-1}$  (September). In the sediments, the mean pH was  
10  $4.29 \pm 0.11$  above the sediment-water interface and increased to  $5.37 \pm 0.28$  at a sediment  
11 depth of 40 to 60 cm. CH<sub>4</sub> concentrations rose with depth from an average of  $10.7 \pm 20.4$   
12  $\mu\text{mol L}^{-1}$  above the sediment-water interface to  $557.3 \pm 72.9 \mu\text{mol L}^{-1}$  at a depth of 40 to  
13 60 cm into the sediment (Fig. 6). The concentration began exceeding theoretical thresholds  
14 for bubble formation at depths between 10 to 40 cm and at a partial pressure of N<sub>2</sub> of 0.8 atm,  
15 but nowhere were concentrations sufficient to form bubbles at 0.5 atm N<sub>2</sub> (Fig. 6). The ave-  
16 rage CO<sub>2</sub> concentration at 40 to 60 cm depth was  $1548.2 \pm 332.5 \mu\text{mol L}^{-1}$  and one order of  
17 magnitude higher than above the sediment-water interface (Fig. 6). Diffusive fluxes towards  
18 the surface water were on average  $10.5 \pm 5.6 \mu\text{mol m}^{-2} \text{h}^{-1}$  (CH<sub>4</sub>) and  $16.9 \pm 9.4 \mu\text{mol m}^{-2} \text{h}^{-1}$   
19 (CO<sub>2</sub>), or  $12.0 \pm 5.6 \mu\text{mol m}^{-2} \text{h}^{-1}$  (CH<sub>4</sub>) and  $25.8 \pm 16.1 \mu\text{mol m}^{-2} \text{h}^{-1}$ , depending on where the  
20 concentration gradient of pore water peeper C is assigned (Fig. 6). *In situ* production and  
21 diffusion from the sediment thus contributed only a small fraction to the CO<sub>2</sub> and CH<sub>4</sub> flux  
22 from the pond. The relative inactivity of the pond sediment was also indicated by the mostly  
23 flat and linear concentration increase of both gases with depth near the sediment-water  
24 interface.

### 25 26 **3.4 Spatial pattern of CH<sub>4</sub> and CO<sub>2</sub> fluxes**

27 Efflux of CH<sub>4</sub> increased 6-fold from open water towards the floating mat and was also much  
28 higher on the floating mat than at the peatland site (Fig. 7 A). The open water median CH<sub>4</sub>  
29 flux of plot p1, p2 and p3, farthest away from the floating mat, was  $0.12 \text{ mmol m}^{-2} \text{h}^{-1}$  and  
30 significantly lower than from plot p4, p5 and p6 closer to the floating mat with a median of  
31  $0.19 \text{ mmol m}^{-2} \text{h}^{-1}$  (Kruskal-Wallis test,  $p < 0.05$ ,  $n = 82$ ) (Supplementary Information, Table  
32 S3). The median CH<sub>4</sub> flux of the floating mat was  $0.64 \text{ mmol m}^{-2} \text{h}^{-1}$  and significantly higher  
33 than the CH<sub>4</sub> flux from the pond (Kruskal-Wallis test,  $p < 0.001$ ,  $n = 243$ ). We observed an  
34 increasing frequency of ebullition and a higher contribution to CH<sub>4</sub> flux towards the floating  
35 mat. On plot p1 only 4 events  $\text{m}^{-2} \text{h}^{-1}$  contributing 5 % occurred, whereas on plot m3 on the  
36 floating mat 168 events  $\text{m}^{-2} \text{h}^{-1}$  contributing 78 % were found (Fig. 7 B and C). The CH<sub>4</sub> flux

1 of m3 was significantly higher than of m1 and m2 (Kruskal-Wallis multiple comparison test,  
2  $p < 0.05$ ,  $n = 84$ ).  
3 The frequency of ebullition and the amount of CH<sub>4</sub> released by bubble events differed along  
4 the transect and in comparison to the peatland site. On the pond, bubble events with a  
5 comparatively small CH<sub>4</sub> release of 0 to 2.5 μmol were most frequent and occurred 5.4 times  
6  $m^{-2} h^{-1}$  (Fig. 8). They also contributed the most to the total CH<sub>4</sub> release. Bubble events  
7 releasing a larger amount of CH<sub>4</sub> were rare. The contribution of ebullition to CH<sub>4</sub> release was  
8 27 %. On the floating mat, CH<sub>4</sub> release by individual bubble events was highly variable with a  
9 maximum of 50 μmol (Fig. 8). Larger bubble events were less frequent than smaller ones.  
10 However, medium and larger bubble events contributed most to CH<sub>4</sub> release with up to 8 %.  
11 The contribution of ebullition to CH<sub>4</sub> release was 66 % on the floating mat. In contrast, it was  
12 only 20 % in the peatland with a clearly different frequency distribution (Fig. 8). Bubble  
13 events occurred over a larger range of release strength than on the pond, but they were less  
14 frequent with a total bubble frequency of only 1.3 events  $m^{-2} h^{-1}$ .  
15 The pond was on average also a net source of CO<sub>2</sub> with a median CO<sub>2</sub> efflux of 1.16  
16  $mmol m^{-2} h^{-1}$  (Fig. 7 D). On the floating mat, daytime ER ranged from 0.53 to 13.45  $mmol$   
17  $m^{-2} h^{-1}$  and maximum NEE from -11.46 to 0.71  $mmol m^{-2} h^{-1}$  (Fig. 7 D).  
18

### 19 **3.5 Controls on CH<sub>4</sub> and CO<sub>2</sub> fluxes**

20 CH<sub>4</sub> and CO<sub>2</sub> fluxes from the pond and ER on the floating mat were significantly negatively,  
21 and maximum NEE on the floating mat positively correlated with air, water and mat  
22 temperature (Table 1 and 2). We found more negative NEE values at an increasing PAR on  
23 the floating mat as well as on the pond. Late summer fluxes of CO<sub>2</sub> and CH<sub>4</sub> across the water-  
24 atmosphere interface were positively correlated with wind speed, whereas the respective mid  
25 summer fluxes were negatively correlated (Table 1 and 2).

26 Total CH<sub>4</sub> fluxes from the floating mat and the pond were significantly higher for periods  
27 with a decreasing air pressure trend over the last 24 h than for periods with an increasing air  
28 pressure trend (Kruskal-Wallis test,  $p < 0.05$  and  $p < 0.01$ ,  $n = 111$  and  $n = 61$ ). At the floating  
29 mat median fluxes during these periods were 0.82 and 0.55  $mmol m^{-2} h^{-1}$ , on the pond 0.13  
30 and 0.04  $mmol m^{-2} h^{-1}$  (see also Supplementary Information, Fig. S4).  
31

### 32 **3.6 Greenhouse gas exchange of the pond system compared to the surrounding peatland**

33 During our daytime measurements the pond and the floating mat were most frequently  
34 significant net sources of CO<sub>2</sub> equivalents, whereas the peatland was generally a sink of CO<sub>2</sub>  
35 equivalents (Fig. 9; Kruskal-Wallis multiple comparison test,  $p < 0.001$ ,  $n = 218$ ). The source  
36 strength of CO<sub>2</sub> equivalents was largest on the floating mat with a median of 0.21 g CO<sub>2</sub>

1 equivalents  $\text{m}^{-2} \text{h}^{-1}$ . While the floating mat and peatland site took up  $\text{CO}_2$  at  $\text{PAR} >$   
2  $1000 \mu\text{mol m}^{-2} \text{s}^{-1}$ , the pond emitted  $\text{CO}_2$  to the atmosphere during 90 % of measurements  
3 (see Figs. 3, 4, 5). When both greenhouse gases were emitted,  $\text{CH}_4$  contributed  $59 \pm 20$  % to  
4 the total emission of  $\text{CO}_2$  equivalents of the pond.

## 7 **4 Discussion**

### 8 **4.1 Spatial pattern of $\text{CH}_4$ and $\text{CO}_2$ fluxes along the peatland – pond ecotone**

9 The peatland and especially the floating mat were summer hot spots of  $\text{CH}_4$  emissions  
10 compared to a variety of sites in other northern peatlands. Fluxes exceeded most, but not all,  
11 emissions reported by Hamilton et al. (1994), Strack et al. (2006), Dinsmore et al. (2009),  
12 Moore et al. (2011), and Trudeau et al. (2013) from similar environments by an order of  
13 magnitude (see also Supplementary Information for a compilation of flux values, Tables S4-  
14 S6). On a per-day and mass basis mean fluxes reached  $204$  and  $437 \text{ mg CH}_4\text{-C m}^{-2} \text{ d}^{-1}$ , which  
15 is at the high end of fluxes reported in meta-analyses (Olefeldt et al., 2013). Average  $\text{CH}_4$   
16 emissions from the open water were still substantial at  $63 \text{ mg CH}_4\text{-C m}^{-2} \text{ d}^{-1}$ , which is about 5  
17 times the flux reported from the multi-year study of Stordalen Mire in Northern Sweden (Wik  
18 et al., 2013). Emissions fell, however, well into the range of fluxes reported from other  
19 peatland ponds (Huttunen et al., 2002; Trudeau et al., 2013; Pelletier et al., 2014). In contrast,  
20  $\text{CO}_2$  fluxes were fairly inconspicuous compared to fluxes in similar systems; on a per-day and  
21 mass basis mean maximum NEE reached  $-5.4 \text{ g CO}_2\text{-C m}^{-2} \text{ d}^{-1}$  in the bog and  $-1.27 \text{ g CO}_2\text{-C}$   
22  $\text{m}^{-2} \text{ d}^{-1}$  on the floating mat, and daytime ER  $3.91 \text{ g CO}_2\text{-C m}^{-2} \text{ d}^{-1}$  and  $1.85 \text{ g CO}_2\text{-C m}^{-2} \text{ d}^{-1}$ ,  
23 respectively. The pond on average emitted  $0.38 \text{ g CO}_2\text{-C m}^{-2} \text{ d}^{-1}$ . Both pond and floating mat  
24 thus lost more  $\text{CO}_2$  than they fixed during the day, which suggests that in both environments  
25 additional  $\text{CO}_2$  was released, for example stemming from carbon-rich groundwater seeping  
26 into the pond.

27 Part of the surprising source strength of methane can be attributed to the inclusion of  
28 ebullition by means of high frequency chamber measurements, similarly as first reported by  
29 Goodrich et al. (2011). Fluxes that are visibly affected by ebullition events have often been  
30 discarded from static chamber fluxes in the past because the non-linearity of concentration  
31 increase over time is problematic when few samples are analyzed by gas chromatography.  
32 Ebullition contributed on average 66 % to the emissions on the floating mat and reached 78 %  
33 at the plot with the highest methane flux (Figs. 4 and 7). The importance and variability of  
34 ebullition was similar as reported from an ombrotrophic peatland in Japan (50 to 64 %;  
35 Tokida et al., 2007). The  $\text{CH}_4$  released by individual bubble events from the floating mat was

1 also on the same order of magnitude as bubble CH<sub>4</sub> release in Sallie's Fen (Goodrich et al.,  
2 2011). At that site the bubble frequency of  $35 \pm 16$  events m<sup>-2</sup> h<sup>-1</sup> was, however, lower than  
3 on the floating mat at Wylde Lake Bog with 54 to 168 events m<sup>-2</sup> h<sup>-1</sup>. In contrast to these  
4 findings, ebullition accounted on average only for 20 % of fluxes at our bog site and 27 % in  
5 the pond (Figs. 3 and 5), where bubble frequency of outer plots was less than 9 events m<sup>-2</sup> h<sup>-1</sup>  
6 and dropped to zero by the end September (Fig. 3). In the pond ebullition was thus less  
7 important than reported previously in 11 lakes in Wisconsin (40 to 60 %; Bastviken et al.,  
8 2004) and two productive, urban ponds in Sweden and China (> 90 %; Natchimuthu et al.,  
9 2014; Xiao et al., 2014).

10 Even though bubbles were rarely observed on p1, p2 and p3 farther away from the floating  
11 mat (Fig. 7) and ceased altogether in September (Fig. 3), formation of CH<sub>4</sub> bubbles may have  
12 initially been possible in the pond sediments. Concentrations exceeded the threshold  
13 concentration of bubble formation at a N<sub>2</sub> partial pressure of 0.8 atm in all locations sampled  
14 (Fig. 6). Such concentrations were only reached at larger sediment depth, though, and  
15 ongoing stripping of N<sub>2</sub> with ebullition may have raised concentration thresholds over time  
16 (Fechner-Levy and Hemond, 1996). At a remaining N<sub>2</sub> partial pressure of 0.5 atm, ebullition  
17 was not possible from a theoretical point of view, which may explain its limited importance in  
18 the pond. The lack of ebullition later on may have been assisted by falling temperatures in  
19 autumn; a change from 20°C to 10°C, for example, raises the threshold for ebullition by 70  
20 μmol L<sup>-1</sup>. Flat or linearly increasing concentration profiles near the sediment-water interface  
21 (Fig. 6) also indicated a lack of active production of the gas in this zone. Concentrations of  
22 CH<sub>4</sub> and CO<sub>2</sub> remained low, typically less than 650 and 1500 μmol L<sup>-1</sup>, respectively,  
23 suggesting that microbial activity in the sediments was limited. Also the diffusive fluxes were  
24 small in units of mass, about 3.5 mg CH<sub>4</sub>-C m<sup>-2</sup> d<sup>-1</sup> and 7.5 mg CO<sub>2</sub>-C m<sup>-2</sup> d<sup>-1</sup>, respectively.  
25 The continuous emission of CH<sub>4</sub> and CO<sub>2</sub> from the pond, on average 63 mg CH<sub>4</sub>-C m<sup>-2</sup> d<sup>-1</sup>  
26 and 380 mg CO<sub>2</sub>-C m<sup>-2</sup> d<sup>-1</sup>, was hence likely driven by respiration in the water column and by  
27 advective inflow of groundwater rich in CH<sub>4</sub> and CO<sub>2</sub>.

28 Our results further suggest that medium and infrequent large bubble events contributed a  
29 substantial fraction to the total CH<sub>4</sub> flux at the floating mat but not in the bog and the pond  
30 (Fig. 8). This was the case even though small bubble events were much more frequent than  
31 large ones (Fig. 8). DelSontro et al. (2015) also reported a strong positive correlation between  
32 ebullition flux and bubble volume in open water and found that the largest 10 % of the  
33 bubbles observed in Lake Wohlen, Switzerland, accounted for 65 % of the CH<sub>4</sub> transport.  
34 According to the authors, large bubbles are disproportionately important because they contain  
35 exponentially more CH<sub>4</sub> with increasing diameter, rise faster, and have less time and a

1 relatively smaller surface area to dissolve or exchange CH<sub>4</sub> with the surroundings (DelSontro  
2 et al., 2015).

3 The decline of CH<sub>4</sub> fluxes, CH<sub>4</sub> bubble frequency and contribution of ebullition from the  
4 floating mat to the open water was striking and fluxes were also considerably higher than at  
5 the peatland site (Fig. 7). These findings emphasize that the floating mats and transition zones  
6 to the open water need to be included when quantifying greenhouse gas budgets of pond and  
7 peatland ecosystems. We cannot mechanistically identify the causes for the observed pattern.  
8 It seems likely that the peak emissions from the floating mat were caused by an optimum of  
9 wet conditions in the peat, favoring methanogenesis and impeding methane oxidation,  
10 presence of some *Carex aquatilis* providing for conduit transport of the gas, and potentially  
11 by a release of methane from groundwater entering the land-water interface. CH<sub>4</sub> flux through  
12 plants with aerenchymatic tissues can be responsible for 50 to 97 % of the total CH<sub>4</sub> flux in  
13 peatlands because the aerenchyma link the anaerobic zone of CH<sub>4</sub> production with the  
14 atmosphere (Kelker and Chanton, 1997; Kutzbach et al., 2004; Shannon et al., 1996).  
15 Kutzbach et al. (2004) found a strong positive correlation between the density of *C. aquatilis*  
16 culms and CH<sub>4</sub> fluxes, as well as a contribution of  $66 \pm 20$  % of the plant-mediated CH<sub>4</sub> flux  
17 through *C. aquatilis* to the total flux in wet polygonal tundra. Since ebullition dominated the  
18 CH<sub>4</sub> flux from the floating mat (Fig. 4) in our particular case this transport mechanism  
19 seemed to be of more limited importance, though. Also recently fixed substrates may have  
20 played a role for high CH<sub>4</sub> emissions from the floating mat. Several studies have found a  
21 positive correlation between the rate of photosynthesis and CH<sub>4</sub> emissions (Joabsson and  
22 Christensen, 2001; Ström et al., 2003), which has been explained by the quick allocation of  
23 assimilated labile carbon to the roots and subsequent exudation to the anaerobic rhizosphere  
24 (Dorodnikov et al., 2011). These recent photosynthates serve as a preferential source of CH<sub>4</sub>  
25 compared to older more recalcitrant organic matter (Chanton et al., 1995). Labile organic  
26 matter produced by vascular plants was probably also imported from the floating mat to the  
27 margin of the pond (Repo et al., 2007; Wik et al., 2013). Given the gradual decline of CH<sub>4</sub>  
28 fluxes along the transect CH<sub>4</sub>-rich groundwater may also have entered the floating mat and  
29 the pond, a process that we did not investigate.

#### 30 31 **4.2 Controls on CH<sub>4</sub> and CO<sub>2</sub> fluxes**

32 In agreement with earlier work air pressure change influenced methane flux. We observed  
33 1.5- to 3-fold higher CH<sub>4</sub> fluxes from the floating mat and the pond during periods of  
34 decreasing compared to increasing air pressure (Supplementary Information, Fig. S4), which  
35 was very likely caused by increased ebullition (Wik et al., 2013). Decreased atmospheric

1 pressure results in bubble expansion, which enhances buoyancy force and entails bubble rise  
2 (Chen and Slater, 2015).

3 The negative correlation of water and mat temperature with CH<sub>4</sub> and CO<sub>2</sub> fluxes from the  
4 pond and CH<sub>4</sub> flux and ER of the floating mat (Table 1 and 2) was unexpected, as it is  
5 consensus that temperature is an important positive control on these fluxes (Pelletier et al.,  
6 2014; Roulet et al., 1997; Sachs et al., 2010; Wik et al., 2014). Also the potential effect of  
7 wind speed on CH<sub>4</sub> and CO<sub>2</sub> fluxes from the pond was ambiguous. Increasing wind speeds  
8 should stimulate the exchange of dissolved gases by increasing turbulence of both air and  
9 water close to the interface (Crusius and Wanninkhof, 2003). Before August 15<sup>th</sup>, wind speed  
10 and CH<sub>4</sub> and CO<sub>2</sub> efflux from the pond were, however, negatively correlated, whereas the  
11 correlation was positive thereafter despite quite consistent wind speed patterns and surface  
12 water CO<sub>2</sub> concentrations throughout the whole study period (Figs. 2 and S2, Supplementary  
13 Information).

14 Both phenomena may be explained by internal biological processes, i.e. the growth and decay  
15 of a dense algal mat on the pond, changing hydrological connection between the pond system  
16 and the surrounding peatland, and the influence of the vascular vegetation on the floating mat.  
17 The algal mat developed in the beginning of July and was largely irreversibly dissolved by a  
18 storm on August 12<sup>th</sup> (Figs. S5 and S6). During its presence CO<sub>2</sub> emissions from the pond  
19 remained low (Fig. 3) and were overestimated by the boundary layer equation approach.  
20 Amplitudes of dissolved CO<sub>2</sub> concentration were strong and concentration decreased with  
21 increasing PAR (Table 1). Such dynamics reflects a strong autochthonous photosynthetic and  
22 respiratory activity and lack of water mixing. The empirical relationship between CO<sub>2</sub>  
23 concentration gradient, wind speed and flux, which is largely controlled by turbulence in the  
24 water column, obviously did not apply under such conditions. The subsequent shift to high  
25 CO<sub>2</sub> and CH<sub>4</sub> emissions was probably partly caused by the decomposition of the remains of  
26 the algal mat, similarly as reported from a boreal and a subtropical pond (Hamilton et al.,  
27 1994; Xiao et al., 2014). Other than that, the algal mat probably represented a physical barrier  
28 to diffusive and ebullitive gas exchange between water column and atmosphere. We observed  
29 trapped gas bubbles within the algal mat with CH<sub>4</sub> concentration of only 4 to 8 %; part of the  
30 originally contained CH<sub>4</sub> may have been re-dissolved and oxidized. Even in shallow lakes and  
31 ponds, CO<sub>2</sub> and CH<sub>4</sub> concentrations can be several-fold higher in the deep water compared to  
32 the surface water during certain periods (Dinsmore et al., 2009; Ford et al., 2002). We can  
33 only assume that such concentration gradients established in or under the algal mat. Its  
34 destruction, mixing of the water column and resuspension of the upper sediment layer  
35 probably entailed the observed peak diffusive CO<sub>2</sub> and CH<sub>4</sub> emissions after the storm on  
36 August 12<sup>th</sup> (Fig. 2, Fig. 3).

1

### 2 **4.3 Relevance of greenhouse gas emissions from the pond system**

3 In terms of radiative forcing, the floating mat and open water behaved differently than the  
4 peatland site during our daytime flux measurements at  $\text{PAR} > 1000 \mu\text{mol m}^{-2} \text{s}^{-1}$ . All three  
5 bog micro-sites represented daytime sinks of  $\text{CO}_2$  equivalents and most so the hummocks  
6 (Fig. 9), which represented about 90 % of the area. The floating mat and to a lesser extent also  
7 the pond were sources of  $\text{CO}_2$  equivalents to the atmosphere, even at daytime, and had a  
8 comparable source strength as the boreal ponds and beaver pond investigated by Hamilton et  
9 al. (1994) and Roulet et al. (1997). Net photosynthetic  $\text{CO}_2$  uptake at light saturation was thus  
10 unable to counterbalance the high  $\text{CH}_4$  emissions of the floating mat in terms of  $\text{CO}_2$   
11 equivalents; at both the floating mat and the pond emission of  $\text{CH}_4$  was more important than  
12  $\text{CO}_2$  exchange in terms of greenhouse gas equivalents. In the pond the average contribution of  
13  $\text{CH}_4$  was 59 %, which is much higher than reported from a beaver pond at the Mer Bleue bog  
14 (5 %; Dinsmore et al., 2009), but comparable to figures from ponds in other studies (36 to  
15 91 %; Hamilton et al., 1994; Huttunen et al., 2002; Pelletier et al., 2014; Repo et al., 2007;  
16 Roulet et al., 1997). We ascribe the large differences between the floating mat and the  
17 peatland site (Figs. 7 and 10) to the influx of allochthonous organic and inorganic carbon to  
18 the pond system from the surroundings and to the different vegetation composition, in  
19 particular the occurrence of *Carex aquatilis* on the floating mat, which may have enhanced  
20  $\text{CH}_4$  production and transport (Kutzbach et al., 2004; Strack et al., 2006). Our results support  
21 earlier suggestions that ponds are important for the greenhouse gas budget of peatlands at  
22 landscape scale (e.g. Pelletier et al. 2014) and they suggest that changes in the area extent of  
23 floating mats and shore length will be an important factor of changes in greenhouse gas  
24 budgets with predicted climate change.

25

### 26 **5 Conclusions**

27 Our summer measurements of atmospheric  $\text{CH}_4$  and  $\text{CO}_2$  exchange revealed a substantial  
28 small-scale spatial variability with 6- and 42-fold increasing median  $\text{CH}_4$  fluxes and bubble  
29 frequencies, respectively, from the open water of the pond towards the surrounding floating  
30 mat. Individual bubble events releasing more than  $10 \mu\text{mol CH}_4$  contributed substantially to  
31 summer  $\text{CH}_4$  emissions from the floating mat, despite their rare occurrence. When  $\text{CH}_4$   
32 emissions of peatlands that contain ponds are quantified, ebullitive and diffusive  $\text{CH}_4$  fluxes  
33 at the land-water interface hence need to be accounted for and the areal cover of the different  
34 microforms and/or plant communities should be thoroughly mapped, as suggested by Sachs et  
35 al. (2010) for tundra landscape. We also observed 4- to 16-fold increases in  $\text{CH}_4$  and  $\text{CO}_2$



1 emissions in late summer that were unrelated to meteorological drivers, such as temperature,  
2 wind speed and radiation. Hydrological connections to adjacent peatlands and internal  
3 hydrological and biological processes, such as the development of algal mats, which can be  
4 abundant in small and shallow water bodies (e.g. Dinsmore et al., 2009; Hamilton et al., 1994;  
5 Xiao et al., 2014) thus require more attention in the future. During our summer daytime flux  
6 measurements, the pond system had a warming effect considering CH<sub>4</sub> and CO<sub>2</sub> exchange,  
7 with the highest net release of CO<sub>2</sub> equivalents from the floating mat. We conclude that  
8 carbon cycling and hydrology of small ponds and their surrounding ecotone need to be further  
9 investigated; these systems are hot spots of greenhouse gas exchange and are likely highly  
10 sensitive to anthropogenic climate change due to their shallowness and dependence on water  
11 budgets and hydrological processes upstream.

12

### 13 **Acknowledgements**

14 The study was financially supported by the German Research Foundation (DFG) grant BL  
15 563/21-1 and an international cooperation grant by the German Academic Exchange Service  
16 (DAAD) to C. Blodau. We thank C. Wagner-Riddle for the possibility to use the former  
17 Blodau laboratory at the School of Environmental Sciences at the University of Guelph and P.  
18 Smith and L. Wing for organizational and technical support. We are grateful to M. Neumann  
19 from the Grand River Conservation Authority for permission to conduct research in the  
20 Luther Marsh Wildlife Management Area, Ontario, Canada, Z. Green for kindly providing  
21 satellite images of the study area and C.A. Lacroix (OAC Herbarium, Biodiversity Institute of  
22 Ontario) for her friendly help in identifying some plants. We are thankful to M. Goebel for  
23 support in the field and advices on study design and data analysis and to Elisa Fleischer for  
24 her helpful comments.

25

26

27

## References

- Bastviken, D., Cole, J.J., Pace, M.L., Tranvik, L.J.: Methane emissions from lakes: Dependence of lake characteristics, two regional assessments, and a global estimate. *Global Biogeochemical Cycles* 18, GB4009, 2004.
- Bastviken, D., Tranvik, L.J., Downing, J.A., Crill, P.M., Enrich-Prast, A.: Freshwater Methane Emissions Offset the Continental Carbon Sink. *Science* 331, 50, 2011.
- Bridgham, S.D., Cadillo-Quiroz, H., Keller, J.K., Zhuang, Q.: Methane emissions from wetlands: biogeochemical, microbial, and modeling perspectives from local to global scales. *Global Change Biology* 19, 1325–1346, 2013.
- Carmichael, M.J., Bernhardt, E.S., Bräuer, S.L., Smith, W.K.: The role of vegetation in methane flux to the atmosphere: should vegetation be included as a distinct category in the global methane budget? *Biogeochemistry* 119, 1–24, 2014.
- Chen, X., Slater, L.: Gas bubble transport and emissions for shallow peat from a northern peatland: The role of pressure changes and peat structure. *Water Resources Research* 51, 151–168, 2015.
- Ciais, P., Sabine, C., Bala, G., Bopp, L., Brovkin, V., Canadell, J., Chhabra, A., DeFries, R., Galloway, J., Heimann, M., Jones, C., Le Quéré, C., Myneni, R.B., Piao, S., Thornton, P.: Carbon and Other Biogeochemical Cycles, in: Stocker, T.F., Qin, D., Plattner, G.-K., Tignor, M., Allen, S.K., Boschung, J., Nauels, A., Xia, Y., Bex, V., Midgley, P.M. (Eds.), *Climate Change 2013: The Physical Science Basis. Contribution of Working Group I to the Fifth Assessment Report of the Intergovernmental Panel on Climate Change*. Cambridge, New York, pp. 465–570, 2013.
- Chanton, J.P., Bauer, J.E., Glaser, P.A., Siegel, D.I., Kelley, C.A., Tyler, S.C., Romanowicz, E.H., Lazrus, A.: Radiocarbon evidence for the substrates supporting methane formation within northern Minnesota peatlands. *Geochimica et Cosmochimica Acta* 59, 3663–3668, 1995.
- Cole, J.J., Prairie, Y.T., Caraco, N.F., McDowell, W.H., Tranvik, L.J., Striegl, R.G., Duarte, C.M., Kortelainen, P., Downing, J.A., Middelburg, J.J., Melack, J.: Plumbing the global carbon cycle: Integrating inland waters into the terrestrial carbon budget. *Ecosystems* 10, 171–184, 2007.

Crusius, J., Wanninkhof, R.: Gas transfer velocities measured at low wind speed over a lake. *Limnology and Oceanography* 48, 1010–1017, 2003.

Davidson, E.A., Savage, K., Verchot, L. V., Navarro, R.: Minimizing artifacts and biases in chamber-based measurements of soil respiration. *Agricultural and Forest Meteorology* 113, 21–37, 2002.

DelSontro, T., McGinnis, D.F., Wehrli, B., Ostrovsky, I.: Size Does Matter: Importance of Large Bubbles and Small-Scale Hot Spots for Methane Transport. *Environmental Science & Technology* 49, 1268–1276, 2015.

Dinsmore, K.J., Billett, M.F., Moore, T.R.: Transfer of carbon dioxide and methane through the soil-water-atmosphere system at Mer Bleue peatland, Canada. *Hydrological Processes* 23, 330–341, 2009.

Dinsmore, K.J., Billett, M.F., Skiba, U.M., Rees, R.M., Drewer, J., Helfter, C.: Role of the aquatic pathway in the carbon and greenhouse gas budgets of a peatland catchment. *Global Change Biology* 16, 2750–2762, 2010.

Dorodnikov, M., Knorr, K.H., Kuzyakov, Y., Wilmking, M.: Plant-mediated CH<sub>4</sub> transport and contribution of photosynthates to methanogenesis at a boreal mire: A <sup>14</sup>C pulse-labeling study. *Biogeosciences* 8, 2365–2375, 2011.

Downing, J.A.: Emerging global role of small lakes and ponds: little things mean a lot. *Limnetica* 29, 9–24, 2010.

Downing, J.A., Cole, J.J., Middelburg, J.J., Striegl, R.G., Duarte, C.M., Kortelainen, P., Prairie, Y.T., Laube, K.A.: Sediment organic carbon burial in agriculturally eutrophic impoundments over the last century. *Global Biogeochemical Cycles* 22, GB1018, 2008.

Drösler, M.: Trace gas exchange and climatic relevance of bog ecosystems, Southern Germany. Doctoral thesis, Technical University of Munich, 2005.

Estop-Aragonés, C., Knorr, K.H., Blodau, C. : Controls on in situ oxygen and DIC dynamics in peats of a temperate fen. *Journal of Geophysical Research*, 117, 2012.

Fechner-Levy, E.J., Hemond, H.F.: Trapped methane volume and potential effects on methane ebullition in a northern peatland. *Limnology and Oceanography* 41, 1375–1383, 1996.

Flessa, H., Rodionov, A., Guggenberger, G., Fuchs, H., Magdon, P., Shibistova, O., Zrazhevskaya, G., Mikheyeva, N., Kasansky, O., Blodau, C.: Landscape controls of CH<sub>4</sub> fluxes in a catchment of the forest tundra ecotone in northern Siberia. *Global Change Biology* 14, 2040–2056, 2008.

Ford, P.W., Boon, P.I., Lee, K.: Methane and oxygen dynamics in a shallow floodplain lake: the significance of periodic stratification. *Hydrobiologia* 485, 97–110, 2002.

Givelet, N., Roos-Barraclough, F., Shoty, W.: Predominant anthropogenic sources and rates of atmospheric mercury accumulation in southern Ontario recorded by peat cores from three bogs: comparison with natural “background” values (past 8000 years). *Journal of Environmental Monitoring* 5, 935–949, 2003.

Goodrich, J.P., Varner, R.K., Frolking, S., Duncan, B.N., Crill, P.M.: High-frequency measurements of methane ebullition over a growing season at a temperate peatland site. *Geophysical Research Letters* 38, L07404, 2011.

Hamilton, J.D., Kelly, C.A., Rudd, J.W.M., Hesslein, R.H., Roulet, N.T.: Flux to the atmosphere of CH<sub>4</sub> and CO<sub>2</sub> from wetland ponds on the Hudson Bay lowlands (HBLs). *Journal of Geophysical Research* 99, 1495–1510, 1994.

Hesslein, R.H.: An in situ sampler for close interval pore water studies. *Limnology and Oceanography* 21, 912–914, 1976.

Huttunen, J.T., Väisänen, T.S., Heikkinen, M., Hellsten, S., Nykänen, H., Nenonen, O., Martikainen, P.J.: Exchange of CO<sub>2</sub>, CH<sub>4</sub> and N<sub>2</sub>O between the atmosphere and two northern boreal ponds with catchments dominated by peatlands or forests. *Plant and Soil* 242, 137–146, 2002.

Joabsson, A., Christensen, T.R.: Methane emissions from wetlands and their relationship with vascular plants: an Arctic example. *Global Change Biology* 7, 919–932, 2001.

Juutinen, S., Alm, J., Martikainen, P., Silvola, J.: Effects of spring flood and water level draw-down on methane dynamics in the littoral zone of boreal lakes. *Freshwater Biology* 46, 855–869, 2001.

Juutinen, S., Rantakari, M., Kortelainen, P.L., Huttunen, J.T., Larmola, T., Alm, J., Silvola, J., Martikainen, P.J.: Methane dynamics in different boreal lake types. *Biogeosciences* 6, 209–223, 2009.

- Juutinen, S., Väiliranta, M., Kuutti, V., Laine, a. M., Virtanen, T., Seppä, H., Weckström, J., Tuittila, E.S.: Short-term and long-term carbon dynamics in a northern peatland-stream-lake continuum: A catchment approach. *Journal of Geophysical Research: Biogeosciences* 118, 171–183, 2013.
- Kelker, D., Chanton, J.: The effect of clipping on methane emissions from *Carex*. *Biogeochemistry* 39, 37–44, 1997.
- Kelly, C.A., Fee, E., Ramlal, P.S., Rudd, J.W.M., Hesslein, R.H., Anema, C., Schindler, E.U.: Natural variability of carbon dioxide and net epilimnetic production in the surface waters of boreal lakes of different sizes. *Limnology and Oceanography* 46, 1054–1064, 2001.
- Kortelainen, P.L., Rantakari, M., Huttunen, J.T., Mattsson, T., Alm, J., Juutinen, S., Larmola, T., Silvola, J., Martikainen, P.J.: Sediment respiration and lake trophic state are important predictors of large CO<sub>2</sub> evasion from small boreal lakes. *Global Change Biology* 12, 1554–1567, 2006.
- Kutzbach, L., Wagner, D., Pfeiffer, E.M.: Effect of microrelief and vegetation on methane emission from wet polygonal tundra, Lena Delta, Northern Siberia. *Biogeochemistry* 69, 341–362, 2004.
- Larmola, T., Alm, J., Juutinen, S., Huttunen, J.T., Martikainen, P.J., Silvola, J.: Contribution of vegetated littoral zone to winter fluxes of carbon dioxide and methane from boreal lakes. *Journal of Geophysical Research: Atmospheres* 109, D19102, 2004.
- Larmola, T., Bubier, J.L., Kobylyanec, C., Basiliko, N., Juutinen, S., Humphreys, E.R., Preston, M., Moore, T.R.: Vegetation feedbacks of nutrient addition lead to a weaker carbon sink in an ombrotrophic bog. *Global Change Biology* 19, 3729–3739, 2013.
- Lerman A.: Chemical exchange across sediment-water interface. *Annual Review of Earth and Planetary Sciences* 6, 281-303, 1978.
- Macrae, M.L., Bello, R.L., Molot, L.A.: Long-term carbon storage and hydrological control of CO<sub>2</sub> exchange in tundra ponds in the Hudson Bay Lowland. *Hydrological Processes* 18, 2051–2069, 2004.
- McEnroe, N.A., Roulet, N.T., Moore, T.R., Garneau, M.: Do pool surface area and depth control CO<sub>2</sub> and CH<sub>4</sub> fluxes from an ombrotrophic raised bog, James Bay, Canada? *Journal of Geophysical Research* 114, G01001, 2009

McLaughlin, J., Webster, K.: Effects of Climate Change on Peatlands in the Far North of Ontario, Canada : A Synthesis. *Arctic, Antarctic and Alpine Research* 46, 84–102, 2014.

Moore, T.R., De Young, A., Bubier, J.L., Humphreys, E.R., Lafleur, P.M., Roulet, N.T.: A Multi-Year Record of Methane Flux at the Mer Bleue Bog, Southern Canada. *Ecosystems* 14, 646–657, 2011.

Michmerhuizen, C.M., Striegl, R.G., McDonald, M.E.: Potential methane emission from north-temperate lakes following ice melt. *Limnology and Oceanography* 41, 985–991, 1996.

Myhre, G., Shindell, D., Bréon, F.-M., Collins, W., Fuglestedt, J., Huang, J., Koch, D., Lamarque, J.-F., Lee, D., Mendoza, B., Nakajima, T., Robock, A., Stephens, G., Takemura, T., Zhang, H.: Anthropogenic and Natural Radiative Forcing, in: Stocker, T.F., Qin, D., Plattner, G.-K., Tignor, M., Allen, S.K., Boschung, J., Nauels, A., Xia, Y., Bex, V., Midgley, P.M. (Eds.), *Climate Change 2013: The Physical Science Basis. Contribution of Working Group I to the Fifth Assessment Report of the Intergovernmental Panel on Climate Change*. Cambridge, New York, pp. 659–740, 2013.

Natchimuthu, S., Panneer Selvam, B., Bastviken, D.: Influence of weather variables on methane and carbon dioxide flux from a shallow pond. *Biogeochemistry* 119, 403–413, 2014.

National Climate Data and Information Archive: Canadian Climate Normals. URL [http://climate.weather.gc.ca/climate\\_normals/index\\_e.html](http://climate.weather.gc.ca/climate_normals/index_e.html) (accessed November 18<sup>th</sup>, 2014).

Olefeldt, D., Turetsky, M.R., Crill P.M., McGuire, A.D.: Environmental and physical controls on northern terrestrial methane emissions across permafrost zones. *Global Change Biology* 19, 589-603, 2013.

Pelletier, L., Strachan, I.B., Garneau, M., Roulet, N.T.: Carbon release from boreal peatland open water pools: Implication for the contemporary C exchange. *Journal of Geophysical Research: Biogeosciences* 119, 207–222, 2014.

R Core Team: *R: A language and environment for statistical computing*. R Foundation for Statistical Computing, Vienna, 2014.

Raymond, P.A., Hartmann, J., Lauerwald, R., Sobek, S., McDonald, C., Hoover, M., Butman, D., Striegl, R.G., Mayorga, E., Humborg, C., Kortelainen, P.L., Dürr, H., Meybeck, M., Ciais, P., Guth, P.: Global carbon dioxide emissions from inland waters. *Nature* 503, 355–359, 2013.

- Repo, M.E., Huttunen, J.T., Naumov, A. V., Chichulin, A. V., Lapshina, E.D., Bleuten, W., Martikainen, P.J.: Release of CO<sub>2</sub> and CH<sub>4</sub> from small wetland lakes in western Siberia. *Tellus* 59B, 788–796, 2007.
- Roulet, N.T., Crill, P.M., Comer, N.T., Dove, A., Boubonniere, R.A.: Flux between a boreal beaver pond and the atmosphere. *Journal of Geophysical Research* 102, 29313–29319, 1997.
- Sachs, T., Giebels, M., Boike, J., Kutzbach, L.: Environmental controls on CH<sub>4</sub> emission from polygonal tundra on the microsite scale in the Lena river delta, Siberia. *Global Change Biology* 16, 3096–3110, 2010.
- Sander, R.: *Compilation of Henry's Law Constants for Inorganic and Organic Species of Potential Importance in Environmental Chemistry*. Max-Planck Institute of Chemistry, Mainz, 1999.
- Sandilands, A.P.: *Annotated Checklist of the Vascular Plants and Vertebrates of Luther Marsh, Ontario*. Ontario Field Biologist, Special Publication No. 2. 1984.
- Shannon, R.D., White, J.R., Lawson, J.E., Gilmour, B.S.: Methane efflux from emergent vegetation in peatlands. *Journal of Ecology* 84, 239–246, 1996.
- Soumis, N., Canuel, R., Lucotte, M.: Evaluation of two current approaches for the measurement of carbon dioxide diffusive fluxes from lentic ecosystems. *Environmental Science and Technology* 42, 2964–2969, 2008.
- Strack, M., Waller, M.F., Waddington, J.M.: Sedge succession and peatland methane dynamics: A potential feedback to climate change. *Ecosystems* 9, 278–287, 2006.
- Ström, L., Ekberg, A., Mastepanov, M., Christensen, T.R.: The effect of vascular plants on carbon turnover and methane emissions from a tundra wetland. *Global Change Biology* 9, 1185–1192, 2003.
- Sugimoto, A., Fujita, N.: Characteristics of methane emissions from different vegetations on a wetland. *Tellus* 49B, 382–392, 1997.
- Tokida, T., Miyazaki, T., Mizoguchi, M., Nagata, O., Takakai, F., Kagemoto, A., Hatano, R.: Falling atmospheric pressure as a trigger for methane ebullition from peatland. *Global Biogeochemical Cycles* 21, GB2003, 2007.
- Tranvik, L.J., Downing, J.A., Cotner, J.B., Loiselle, S.A., Striegl, R.G., Ballatore, T.J., Dillon, P., Finlay, K., Fortino, K., Knoll, L.B., Kortelainen, P.L., Kutser, T., Larsen, S.,

Laurion, I., Leech, D.M., McCallister, S.L., Mcknight, D.M., Melack, J.M., Overholt, E., Porter, J.A., Prairie, Y.T., Renwick, W.H., Roland, F., Sherman, B.S., Schindler, D.W., Sobek, S., Tremblay, A., Vanni, M.J., Verschoor, A.M., Wachenfeldt, E. Von, Weyhenmeyer, G.A.: Lakes and reservoirs as regulators of carbon cycling and climate. *Limnology and Oceanography* 54, 2298–2314, 2009.

Trudeau, N.C., Garneau, M., Pelletier, L.: Methane fluxes from a patterned fen of the northeastern part of the La Grande river watershed, James Bay, Canada. *Biogeochemistry* 113, 409–422, 2013.

Turunen, J., Tomppo, E., Tolonen, K., Reinikainen, A.: Estimating carbon accumulation rates of undrained mires in Finland – application to boreal and subarctic regions. *The Holocene* 12, 69–80, 2002.

Varadharajan, C., Hemond, H.F.: Time-series analysis of high-resolution ebullition fluxes from a stratified, freshwater lake. *Journal of Geophysical Research: Biogeosciences* 117, G02004, 2012.

Verpoorter, C., Kutser, T., Seekell, D.A., Tranvik, L.J.: A global inventory of lakes based on high-resolution satellite imagery. *Geophysical Research Letters* 41, 6396–6402, 2014.

Walter, K.M., Zimov, S.A., Chanton, J.P., Verbyla, D., Chapin, F.S.: Methane bubbling from Siberian thaw lakes as a positive feedback to climate warming. *Nature* 443, 71–75, 2006.

Wik, M., Crill, P.M., Varner, R.K., Bastviken, D.: Multiyear measurements of ebullitive methane flux from three subarctic lakes. *Journal of Geophysical Research: Biogeosciences* 118, 1307–1321, 2013.

Wik, M., Thornton, B.F., Bastviken, D., MacIntyre, S., Varner, R.K., Crill, P.M.: Energy input is primary controller of methane bubbling in subarctic lakes. *Geophysical Research Letters* 41, 555–560, 2014.

Xenopoulos, M.A., Lodge, D.M., Frenress, J., Kreps, T.A., Bridgham, S.D., Grossman, E., Jackson, C.J.: Regional comparisons of watershed determinants of dissolved organic carbon in temperate lakes from the Upper Great Lakes region and selected regions globally. *Limnology and Oceanography* 48, 2321–2334, 2003.

Xiao, S., Yang, H., Liu, D., Zhang, C., Lei, D., Wang, Y., Peng, F., Li, Y., Wang, C., Li, X., Wu, G., Liu, L.: Gas transfer velocities of methane and carbon dioxide in a subtropical shallow pond. *Tellus* 66B, 23795, 2014.





Table 1. Correlations of CH<sub>4</sub> and CO<sub>2</sub> fluxes of the pond with environmental variables. CH<sub>4</sub> flux comprises both ebullition and diffusion if not annotated otherwise.

Flux	Time period	Spearman's rho	P	n
<i>mean air temperature since sunrise</i>				
CO <sub>2</sub>	whole period	- 0.54	< 0.001	147
CH <sub>4</sub>	whole period	- 0.36	< 0.001	147
diffusive CH <sub>4</sub> <sup>a</sup>	whole period	- 0.67	< 0.001	119
<i>mean water temperature during measurements</i>				
CO <sub>2</sub>	whole period	- 0.47	< 0.001	94
CH <sub>4</sub>	whole period	- 0.50	< 0.001	94
diffusive CH <sub>4</sub> <sup>a</sup>	whole period	- 0.60	< 0.001	82
<i>mean PAR of the last 3 h</i>				
CO <sub>2</sub>	whole period	- 0.49	< 0.001	147
<i>mean wind speed of the last 24 h</i>				
CO <sub>2</sub>	mid summer <sup>b</sup>	- 0.35	< 0.05	43
CO <sub>2</sub>	late summer <sup>c</sup>	+ 0.45	< 0.001	104
CO <sub>2</sub>	whole period	not significant		
CH <sub>4</sub>	mid summer <sup>b</sup>	- 0.35	< 0.05	43
CH <sub>4</sub>	late summer <sup>c</sup>	+ 0.63	< 0.001	104
CH <sub>4</sub>	whole period	+ 0.26	< 0.01	147
<i>maximum wind speed of the last 24 h</i>				
CO <sub>2</sub>	mid summer <sup>b</sup>	- 0.45	< 0.01	43
CO <sub>2</sub>	late summer <sup>c</sup>	+ 0.35	< 0.001	104
CO <sub>2</sub>	whole period	+ 0.17	< 0.05	147
CH <sub>4</sub>	mid summer <sup>b</sup>	- 0.55	< 0.001	43
CH <sub>4</sub>	late summer <sup>c</sup>	+ 0.63	< 0.001	104
CH <sub>4</sub>	whole period	+ 0.32	< 0.001	147

<sup>a</sup>: only measurements without ebullition included

<sup>b</sup>: July 10<sup>th</sup> to August 7<sup>th</sup>

<sup>c</sup>: August 15<sup>th</sup> to September 29<sup>th</sup>

Table 2. Correlations of CH<sub>4</sub> and CO<sub>2</sub> fluxes of the floating mat with environmental variables. CH<sub>4</sub> flux comprises both ebullition and diffusion if not annotated otherwise

Flux	Time period	Spearman's rho	P	n
<i>mean air temperature since sunrise</i>				
max. NEE	whole period	+ 0.74	< 0.001	20
CH <sub>4</sub>	whole period	- 0.42	< 0.001	79
<i>mean mat temperature during measurements</i>				
ER	whole period	- 0.44	< 0.01	38
CH <sub>4</sub>	whole period	- 0.41	< 0.001	79
diffusive	whole period	- 0.52	< 0.001	53
CH <sub>4</sub> <sup>a</sup>				
<i>mean PAR during measurements</i>				
NEE	mid summer <sup>b</sup>	not significant		
NEE	late summer <sup>c</sup>	- 0.60	< 0.01	26
NEE	whole period	- 0.37	< 0.05	42

<sup>a</sup>: only measurements without ebullition included

<sup>b</sup>: July 10<sup>th</sup> to August 7<sup>th</sup>

<sup>c</sup>: August 15<sup>th</sup> to September 29<sup>th</sup>

## Figures

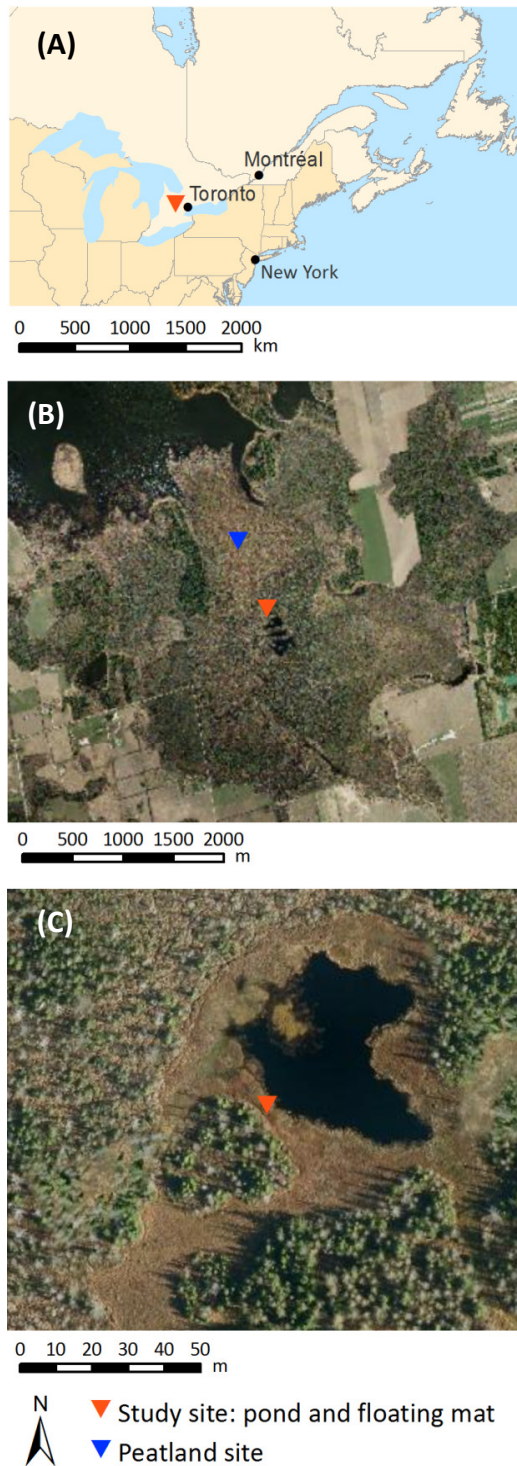


Figure 1. Location of the study site in southern Ontario, Canada (panel A), studied pond with floating mat and peatland site in Wylde Lake Bog in the Luther Marsh Wildlife Management Area with Luther Lake in the northwest (panel B) and close-up of the studied pond and floating mat (panel C) (Grand River Conservation Authority, 2010)

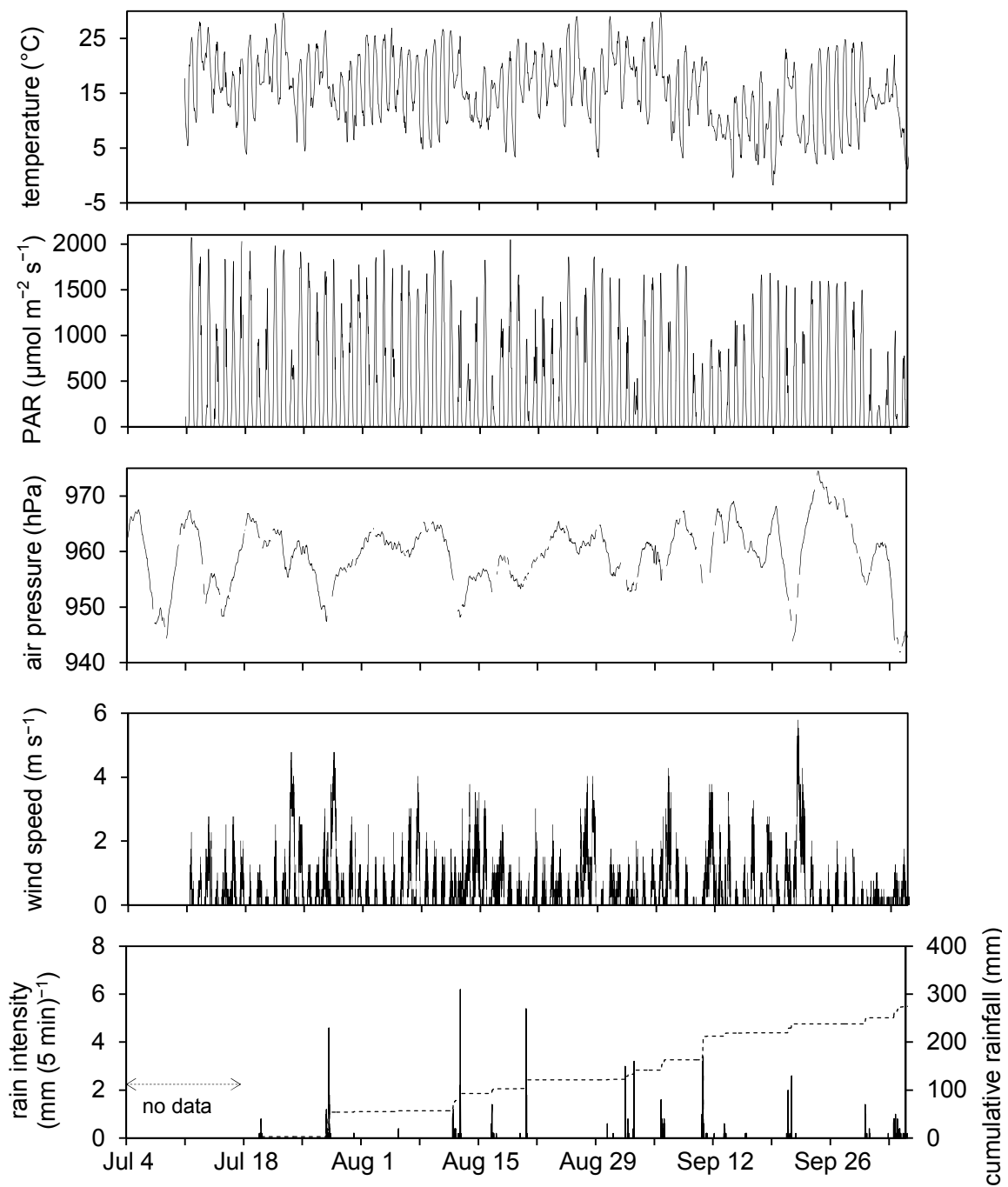


Figure 2. Time series of weather variables at the study site. Air temperature, photosynthetically active radiation (PAR) and air pressure are shown as hourly means, wind speed and rain intensity as 5 min averages. The dashed line in the lowest panel shows the cumulative rainfall.

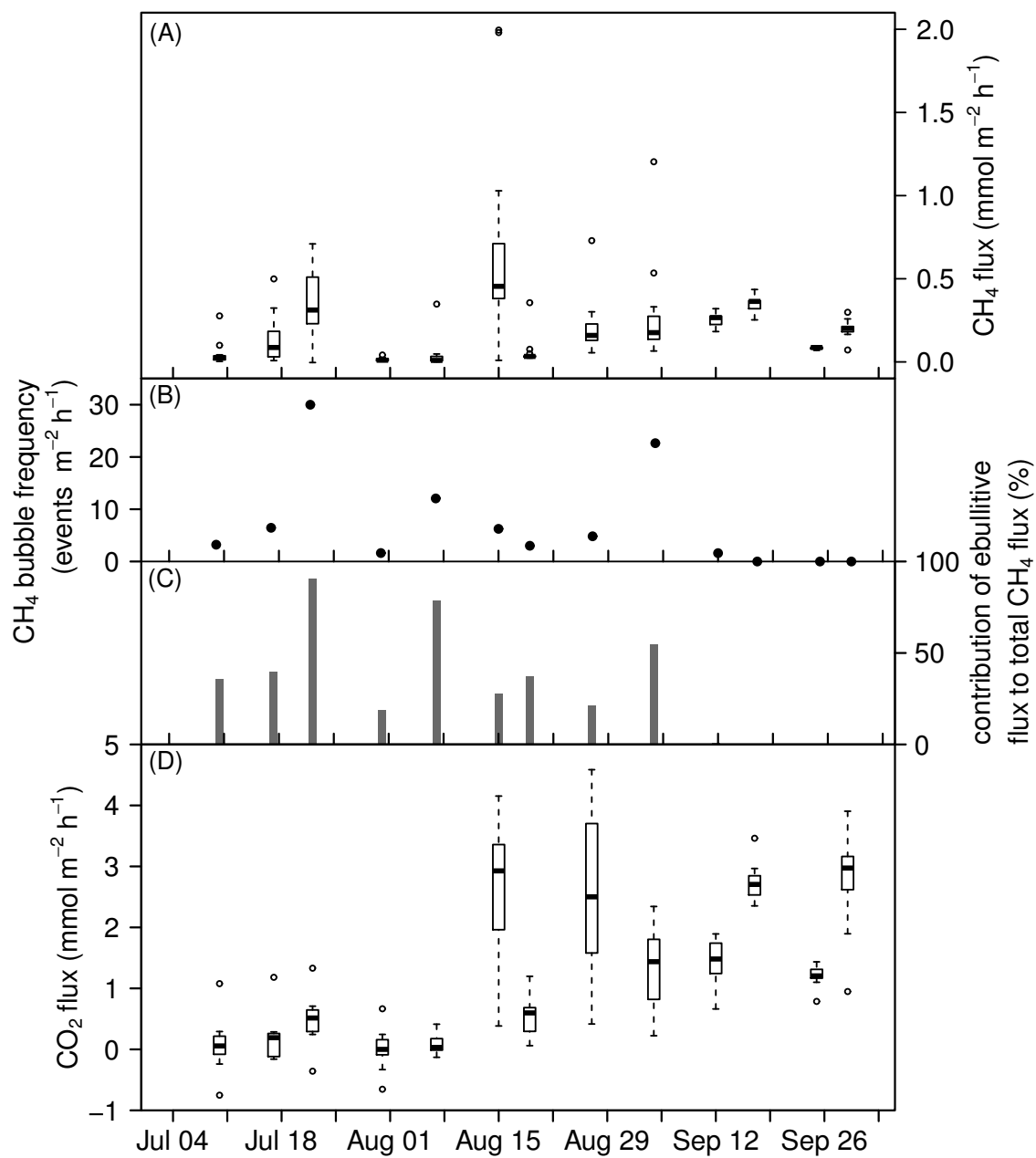


Figure 3. Time series of pond CH<sub>4</sub> fluxes (panel A), CH<sub>4</sub> bubble frequency (panel B), contribution of ebullitive CH<sub>4</sub> flux to total CH<sub>4</sub> flux (panel C) and CO<sub>2</sub> fluxes (panel D) on measuring days from July 10<sup>th</sup> until September 29<sup>th</sup>, 2014. In panel (A) and (D), the bold horizontal line shows the median, the bottom and the top of the box the 25<sup>th</sup> and 75<sup>th</sup> percentile and the whiskers include all values within 1.5 times the interquartile range.

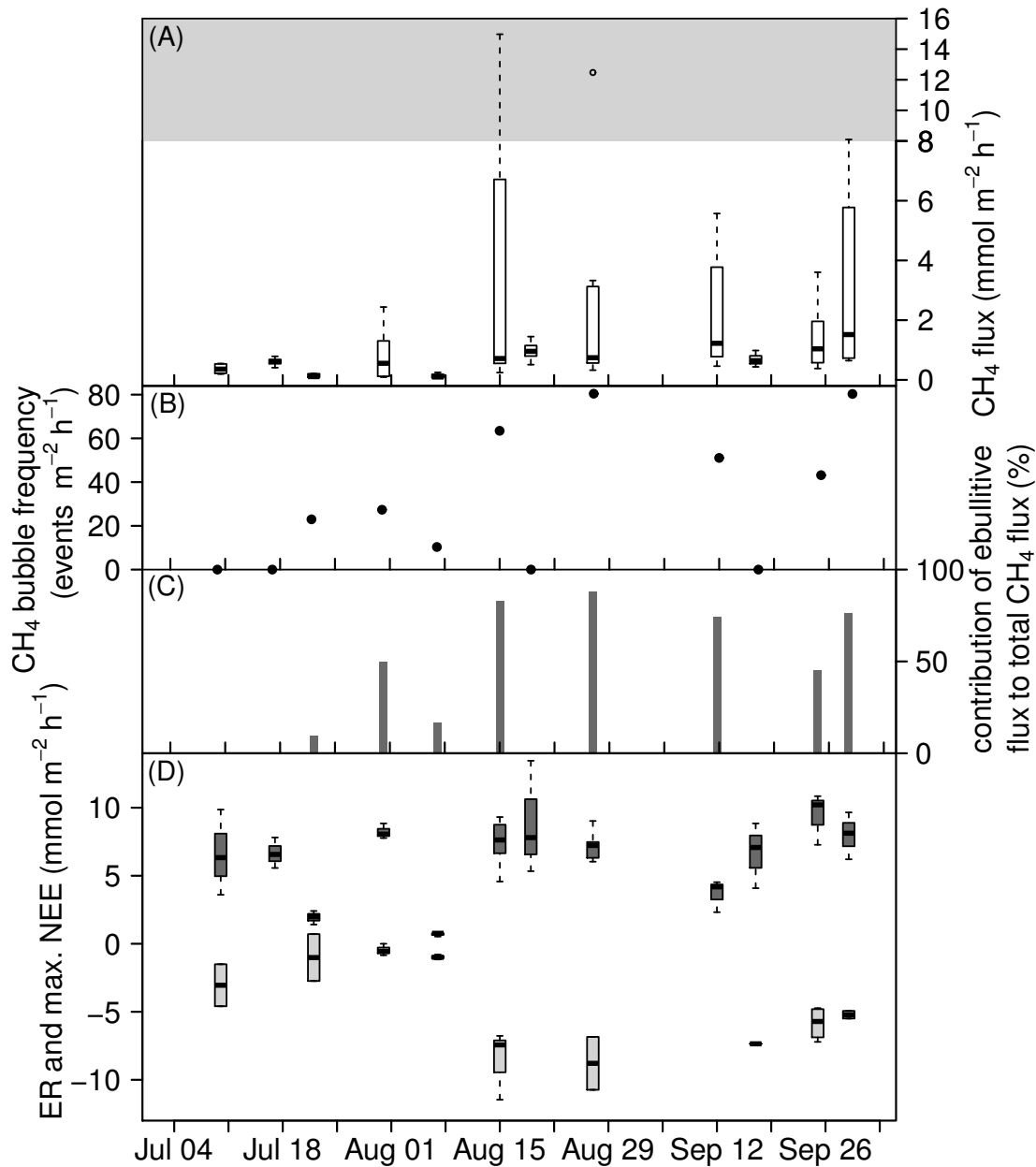


Figure 4. Time series of floating mat CH<sub>4</sub> fluxes (panel A), CH<sub>4</sub> bubble frequency (panel B), contribution of ebullitive CH<sub>4</sub> flux to total CH<sub>4</sub> flux (panel C) as well as ecosystem respiration (ER) and maximum net ecosystem exchange (NEE) (panel D) on measuring days from July 10<sup>th</sup> until September 29<sup>th</sup>, 2014. Note the different scaling of the y-axis within the gray area in panel (A). In panel (D), the dark gray boxes show the daytime ER and the light gray boxes the maximum net ecosystem exchange at values of photosynthetically active radiation > 1000  $\mu\text{mol m}^{-2} \text{s}^{-1}$ . In panel (A) and (D), the bold horizontal line shows the median, the bottom and the top of the box the 25<sup>th</sup> and 75<sup>th</sup> percentile and the whiskers include all values within 1.5 times the interquartile range.

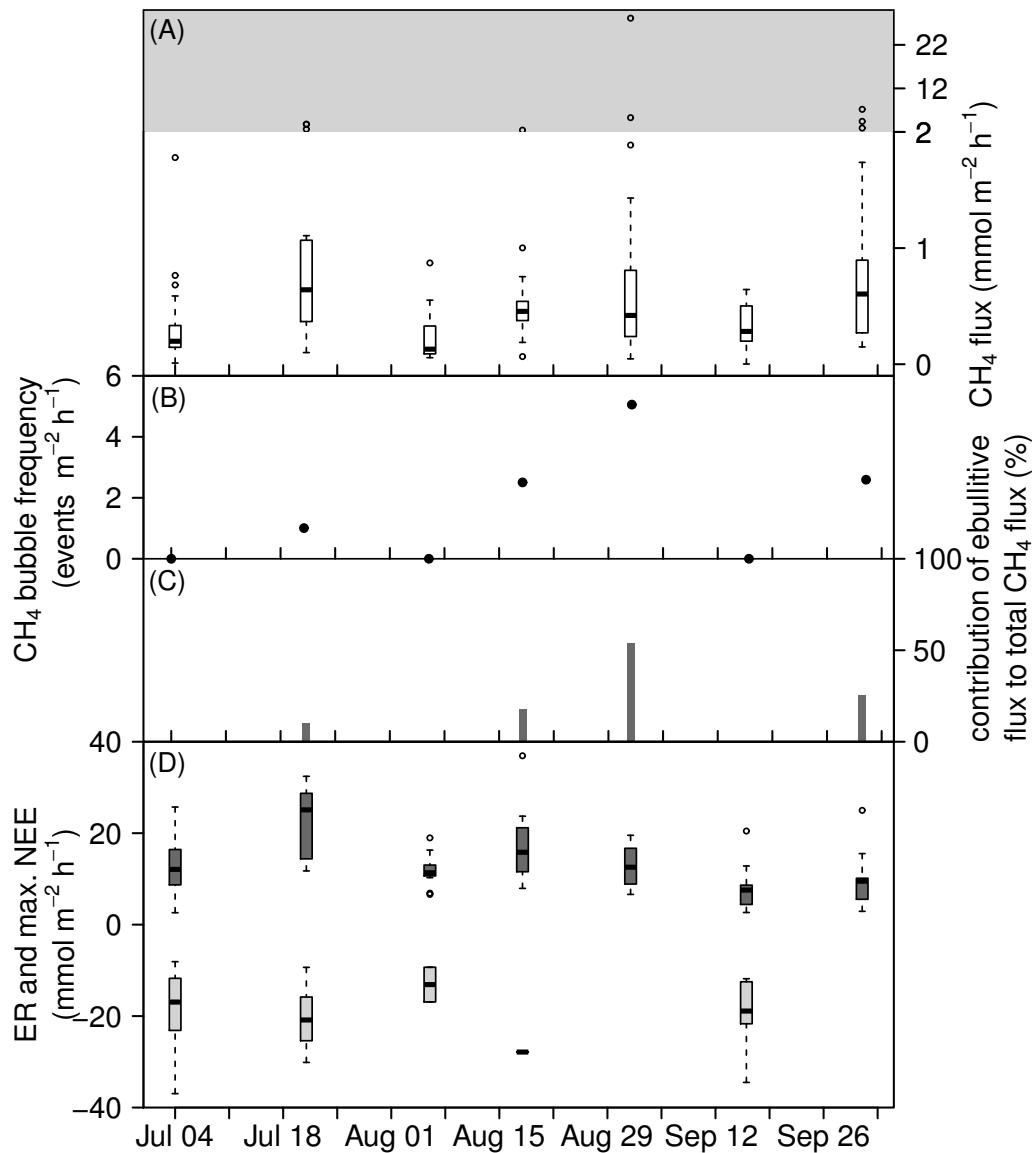


Figure 5: Time series of peatland CH<sub>4</sub> fluxes (panel A), CH<sub>4</sub> bubble frequency (panel B), contribution of ebullitive CH<sub>4</sub> flux to total CH<sub>4</sub> flux (panel C) as well as ecosystem respiration (ER) and maximum net ecosystem exchange (NEE) (panel D) on measuring days from July 4<sup>th</sup> until October 1<sup>st</sup>, 2014. Note the different scaling of the y-axis within the gray area in panel (A). In panel (D), the dark gray boxes show the daytime ER and the light gray boxes the maximum net ecosystem exchange at values of photosynthetically active radiation > 1000  $\mu\text{mol m}^{-2} \text{s}^{-1}$ . In panel (A) and (D), the bold horizontal line shows the median, the bottom and the top of the box the 25<sup>th</sup> and 75<sup>th</sup> percentile and the whiskers include all values within 1.5 times the interquartile range.



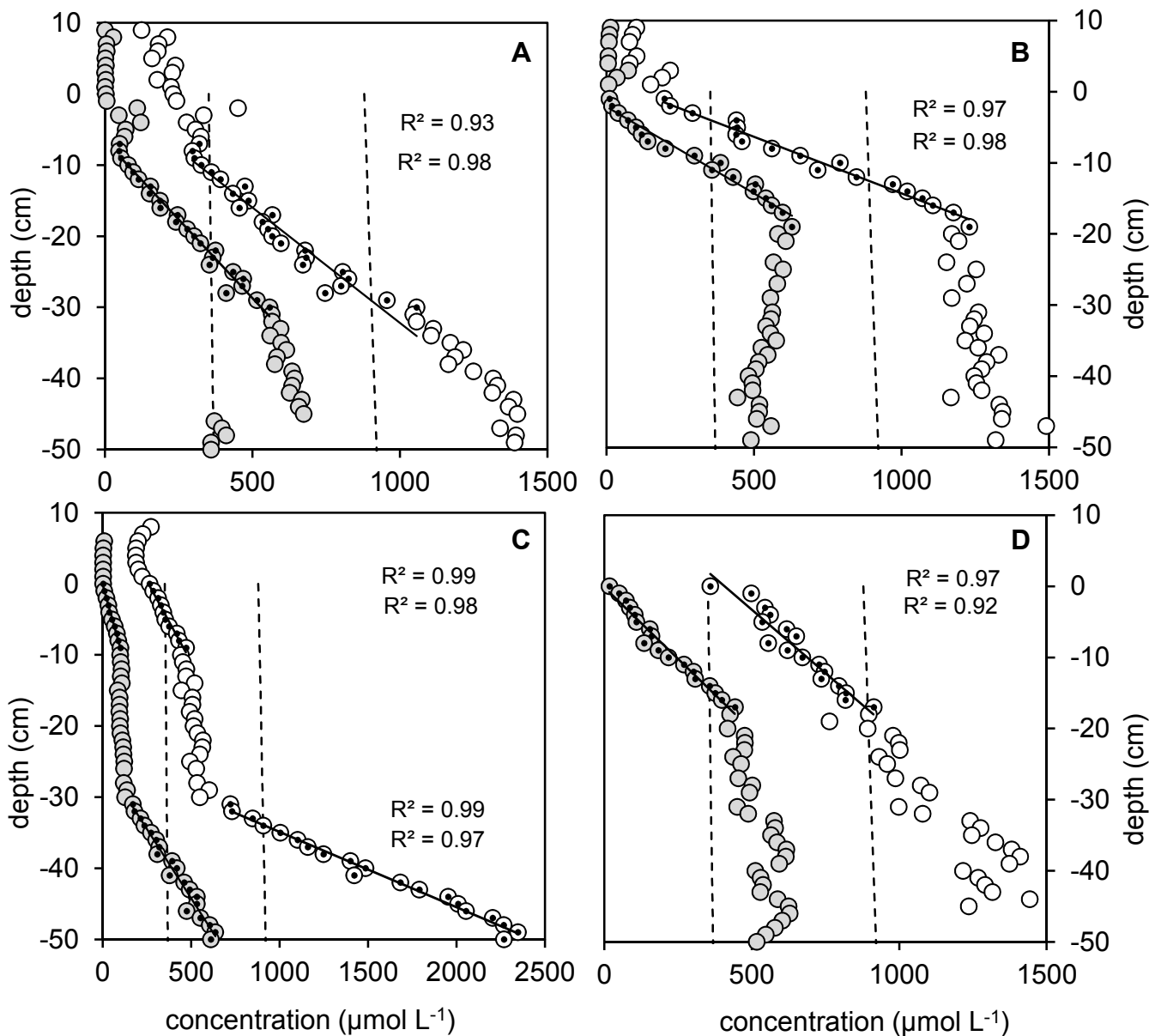


Figure 6:  $\text{CH}_4$  (shaded symbols) and  $\text{CO}_2$  (open symbols) concentrations near the sediment-water interface and in the sediment of the pond in four locations (A – D) on September 25<sup>th</sup> and 29<sup>th</sup>, respectively, as obtained with porewater peepers. Water depth at the locations was about 0.5 meters; a depth of zero on the y-axis indicates the assumed sediment-water interface. Black lines represent regression slopes (with regression coefficient  $R^2$ ) used to calculate diffusive fluxes towards the sediment-water interface. Dashed lines denote depth and temperature dependent theoretical thresholds for formation of  $\text{CH}_4$  bubbles at 0.8 atm (lower line) and 0.5 atm (upper line) partial pressure of  $\text{N}_2$  in the pond sediment at 15°C. In panel C also the diffusive flow from deeper sediment layers was calculated.

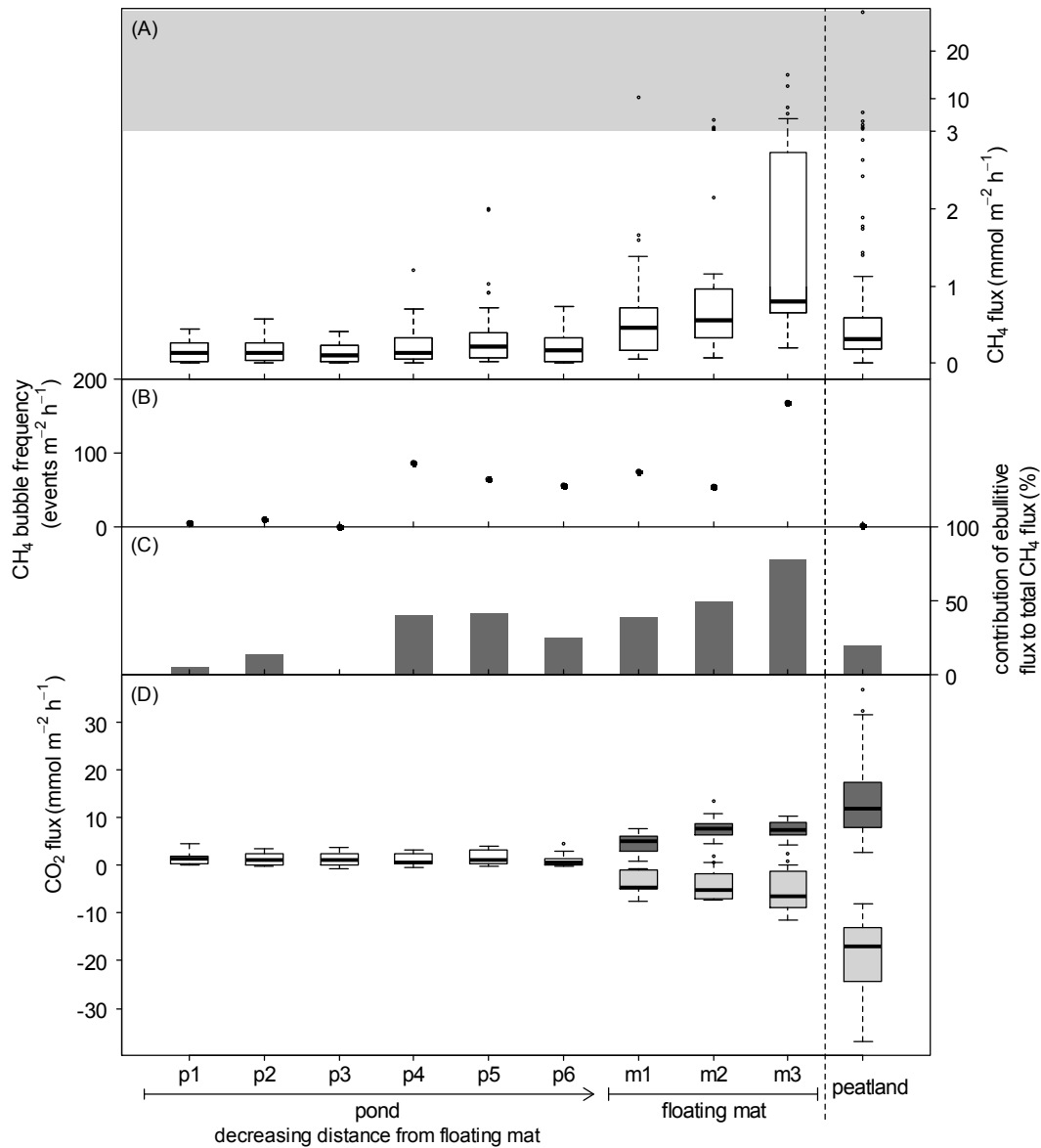


Figure 7: CH<sub>4</sub> fluxes (panel A), CH<sub>4</sub> bubble frequency (panel B), contribution of ebullitive CH<sub>4</sub> flux to total CH<sub>4</sub> flux (panel C) and CO<sub>2</sub> fluxes (panel D) of the pond (p1 to p6) along a gradient of decreasing distance from the floating mat, of the 3 measuring plots on the floating mat (m1 to m3) and of the peatland site for comparison. Note the different scaling of the y-axis within the gray area in panel (A). In panel (D), the transparent boxes show the net CO<sub>2</sub> flux of the pond, the dark gray boxes the daytime ER and the light gray boxes the maximum net ecosystem exchange of the floating mat and the peatland at values of photosynthetically active radiation > 1000  $\mu\text{mol m}^{-2} \text{s}^{-1}$ . In panel (A) and (D), the bold horizontal line shows the median, the bottom and the top of the box the 25<sup>th</sup> and 75<sup>th</sup> percentile and the whiskers include all values within 1.5 times the interquartile range.

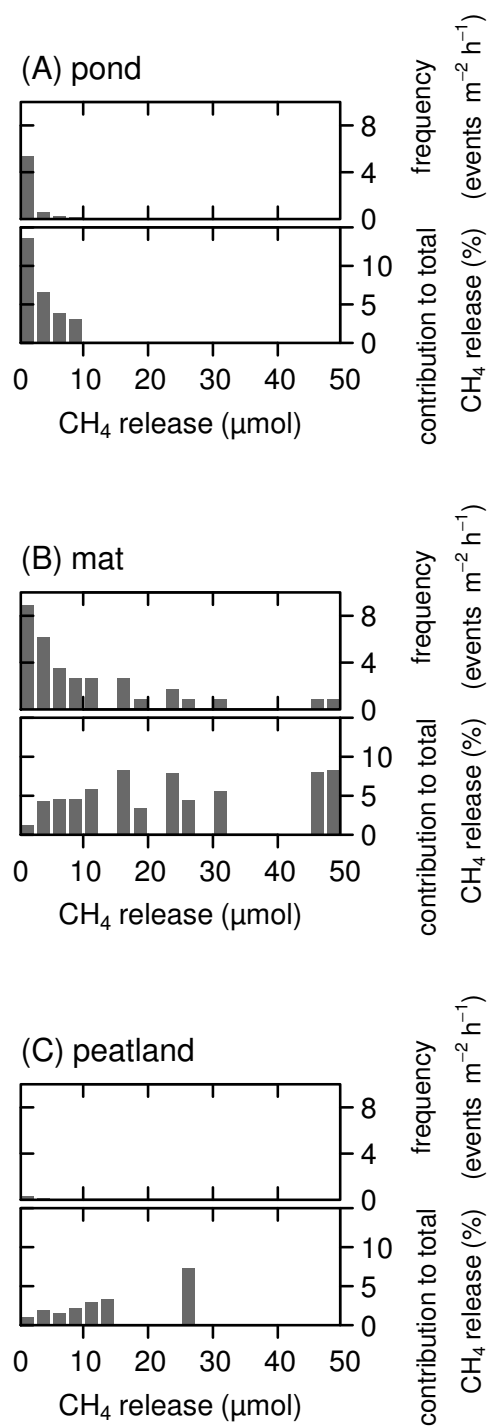


Figure 8: Frequency distribution of ebullitive CH<sub>4</sub> release (upper panels) as well as contribution of each size group of ebullitive CH<sub>4</sub> release to the total CH<sub>4</sub> release (lower panels) of the pond (panel A), the floating mat (panel B) and the peatland (panel C).

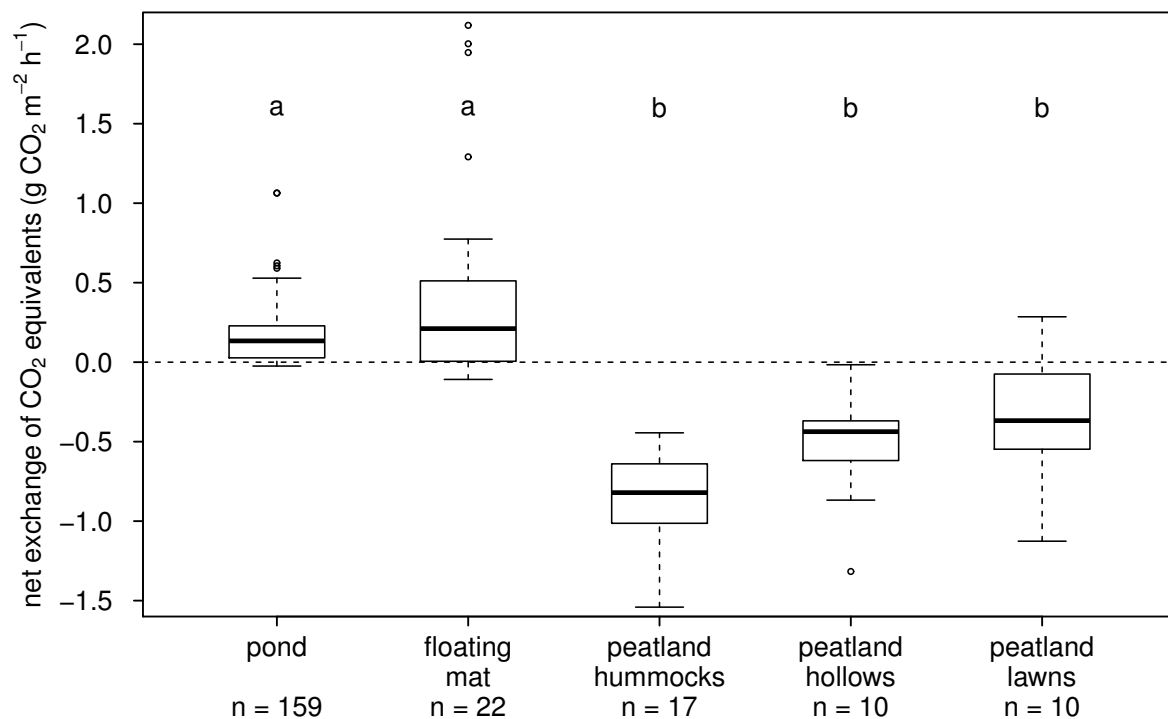


Figure 9: Daytime net exchange of CO<sub>2</sub> equivalents of the pond, the floating mat and the three different microforms of the peatland. Different letters indicate significant differences (Kruskal-Wallis multiple comparison test,  $p < 0.001$ ,  $n = 218$ ). For comparability of the CO<sub>2</sub> fluxes of the floating mat and the peatland, only maximum net ecosystem exchange at values of photosynthetically active radiation  $> 1000 \mu\text{mol m}^{-2} \text{s}^{-1}$  was used for the calculation. The bold horizontal line shows the median, the bottom and the top of the box the 25<sup>th</sup> and 75<sup>th</sup> percentile and the whiskers include all values within 1.5 times the interquartile range.